Global Warming

Humans are taking organic C, long buried within the ⊕, pumping it out as petroleum or mining it as coal, burning it & releasing CO_2 to the atmosphere.

This has happened significantly only in past ~ 100 years — the industrial revolution

Current rate of CO_2 production due to fossil fuel consumption is

5.5 Gt/yr

This includes a small fraction due to cement production

limestone $CaCO_3$ $\xrightarrow{\text{heat}}$ $CaO + CO_2$ ↑ to atmosphere

lime or cement

$CaO + H_2O \rightarrow Ca(OH)_2$

concrete (e.g. floor of Room 10)

Fig. 11.18 (Holland & Petersen) history of CO_2 release by humans past 130–140 yrs (since industrial revolution.

For comparison recall that natural CO_2 cycle involves ~ 65 GtC/yr fixation by

photosynthesis & respiration by bacteria, etc.

Human fossil fuel consumption ~ 10% perturbation.

First was Svante Arrhenius

~~First person~~ one of first people to think about environmental consequences of this — Roger Revelle — then at UCSD

1958 — suggested to Charles Keeling to try to measure — established observatory at Mauna Loa, Hawaii — high above vegetation ⇒ [redacted] average CO_2 ~ unaffected by photosynthesis.

Continuous record since that time — possibly most famous time series in geosciences.

Annual fluctuations ± 3 ppm due to seasonal cycle of photosynthesis

Superimposed on long-term increase from 316 ppm in 1958 to [redacted] 360 ppm in 1996 — average 1.2 ppm/yr.

clear evidence of [redacted] increase in accumulation rate

1.5 ppm/yr or 0.4% currently

[redacted] $\frac{1.5}{360} = 0.4\%$

This famous record has led to intensive study of this phenomenon during the past decade.

Other observatories (e.g. SPA) established.

CO_2 increase found to be a global phenomenon.

Extension of record into the past.

Drilling of ice cores in Greenland & Antarctica

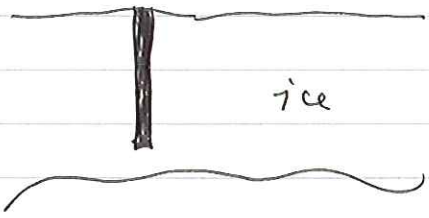

Known ice accumulation rate gives chronology (cm/yr).

Measure % CO_2 in trapped air bubbles in ice.

Melt ice — collect trapped air — measure % CO_2

Pre-industrial level ~ 280 ppm

Keeling Mauna Loa measurements began 1958 — already 315 ppm

Clear evidence of exponential growth.

What is current growth rate in GtC/yr?

(0.0042)(760 GtC in atmosphere)

= 3.2 GtC/yr

↑ observed rate of increase

Increase in growth rate from ~1 ppm/yr to ~1.5 ppm/yr in past 40 yrs.

We also know very well the rate at which we are adding CO_2 to the atmosphere by fossil fuel burning and — to a much lesser extent — cement production

5.5 GtC/yr ← emission rate

This discrepancy has come to be known as the <u>missing carbon problem</u>

Fossil fuel consumption is releasing ~50% more CO_2 to atmosphere than we see — why?

Our current understanding of the <u>global</u> carbon budget is as follows:

fossil fuels & cement	5.5 GtC/yr
tropical deforestation	1.6 GtC/yr
Total anthropogenic emissions	7.1 GtC/yr

Discrepancy even larger!

Two sinks have been determined with greater certainty by recent work:

(1) uptake by oceans — Jorge Sarmiento (Princeton)

↓ CO_2

↓ CO_2 into mixed layer

phytoplankton

$CO_2 + H_2O \rightarrow CH_2O + O_2$

↓ die & sink (biological pump)

↓ slow transport into deep oceans ~ 1000 yr timescale (thermohaline circulation)

also sinking of cold CO_2 rich water

Ocean uptake cannot be measured. Must be modelled. Best estimate

2.0 GtC/yr into oceans

example — no virgin forest in Princeton area but lots of 2d growth

people used to burn wood for fuel & be much more reliant upon local agriculture

Finally, just in past 2-3 years:

Northern hemisphere forest regrowth
e.g. Princeton — my backyard

0.5 GtC/yr

Net effect of land-use changes: 1.6 − 0.5 = 1.1 GtC/yr

Net imbalance 1.4 ± 1.5 GtC/yr

Maybe zero within errors.

Many suggestions:

(1) CO_2 fertilization — plants need CO_2 — increased concentration in atmosphere has stimulated growth

(3) northern forest regrowth may still be underestimated

How much would we need?

$$\frac{1.4}{65} = 2\%$$

↑ NPP

(2) nitrogen fertilization — excess nitrate from farmers' fields has fertilized phytoplankton production

Five years ago, missing C problem thought to be very important — now:

- new sink found
- no dearth of explanations for remaining discrepancy
- ~~1.4~~ 1.4 ± 1.5 — big deal anyway.

The anthropogenic increase in atmospheric CO_2 from 280 ppm to 360 ppm today has increased the "thickness" of the greenhouse "glass" slightly.

How much? Enough to increase the re-radiated IR by 1.6 W/m^2 (see Fig. 3

Other activities have also affected the radiative forcing

Methane & other greenhouse gases — sources of methane: rice paddies, bovine flatulence, natural gas leakage

Halocarbons — refrigerants (CFC) more notorious for their role in destroying polar stratospheric ozone

Also human release of aerosols — cause increased scattering ⇒ slight increase in albedo by ~ 0.3%

$$-(.003)(340\ W/m^2) \approx -1\ W/m^2$$

Total anthropogenic effect ~ 2 W/m^2 increase with large error bars

Sarmiento et al. (1998) study

Inverted ~ 60 atmospheric CO_2 trends for 3 uptake sources.

Need to model inputs (well known), ocean uptake, redistribution by mean winds, forest cover, ...

Find NA uptake 1.7 GtC/yr

In conflict with US Forest Service inventories — only 0.2 – 0.3 GtC/yr.

Controversial — US emissions are 1.6 GtC/yr — would ⇒ US is break-even — no need for emission controls.

Strong tradeoff with NA – Eurasian takeup.
Reason: result relies on weak EW trends (which are smoothed by zonal winds)

but these is not

Map shows theoretical anomaly in absence of takeup — should be an excess of atmospheric CO_2 over NA because of emissions

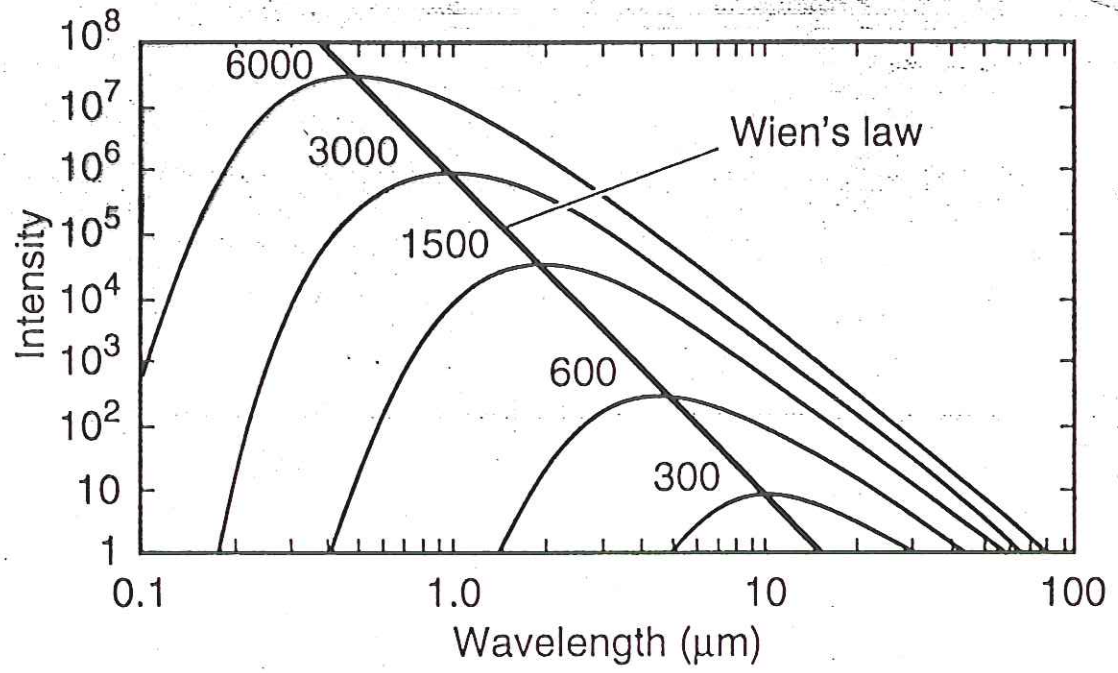

Figure 3.7 Blackbody radiation spectra as a function of temperature (kelvin), over the entire range of temperatures relevant to environmental studies. The values are displayed here on a log-log graph, so that both the wavelength and intensity scales are greatly compressed and cover many orders of magnitude.

Figure 3.8 The relative spectra of sunlight and Earth's blackbody radiation (referred to as terrestrial radiation or Earthglow). The spectral regions of the emissions are seen to be quite distinct, with little overlap of spectra.

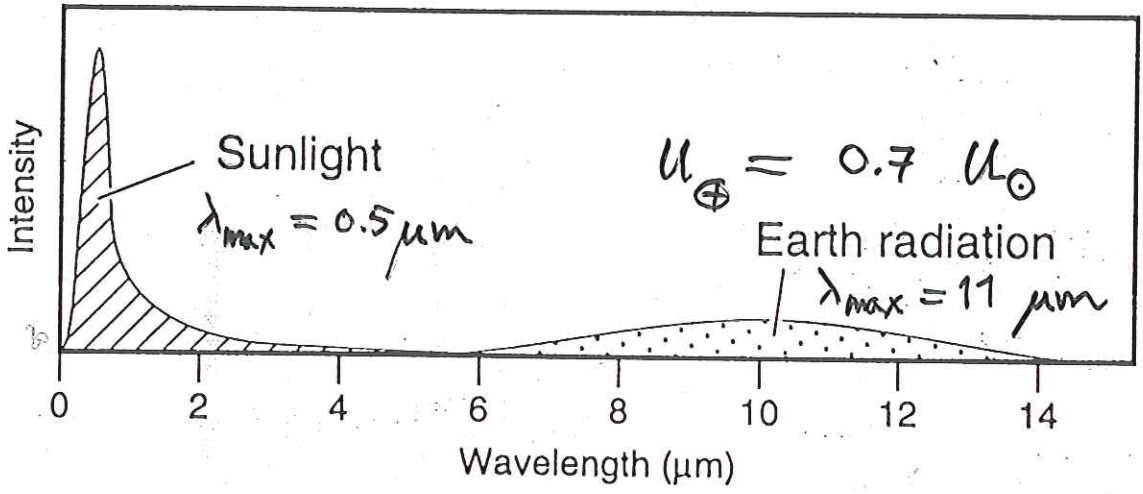

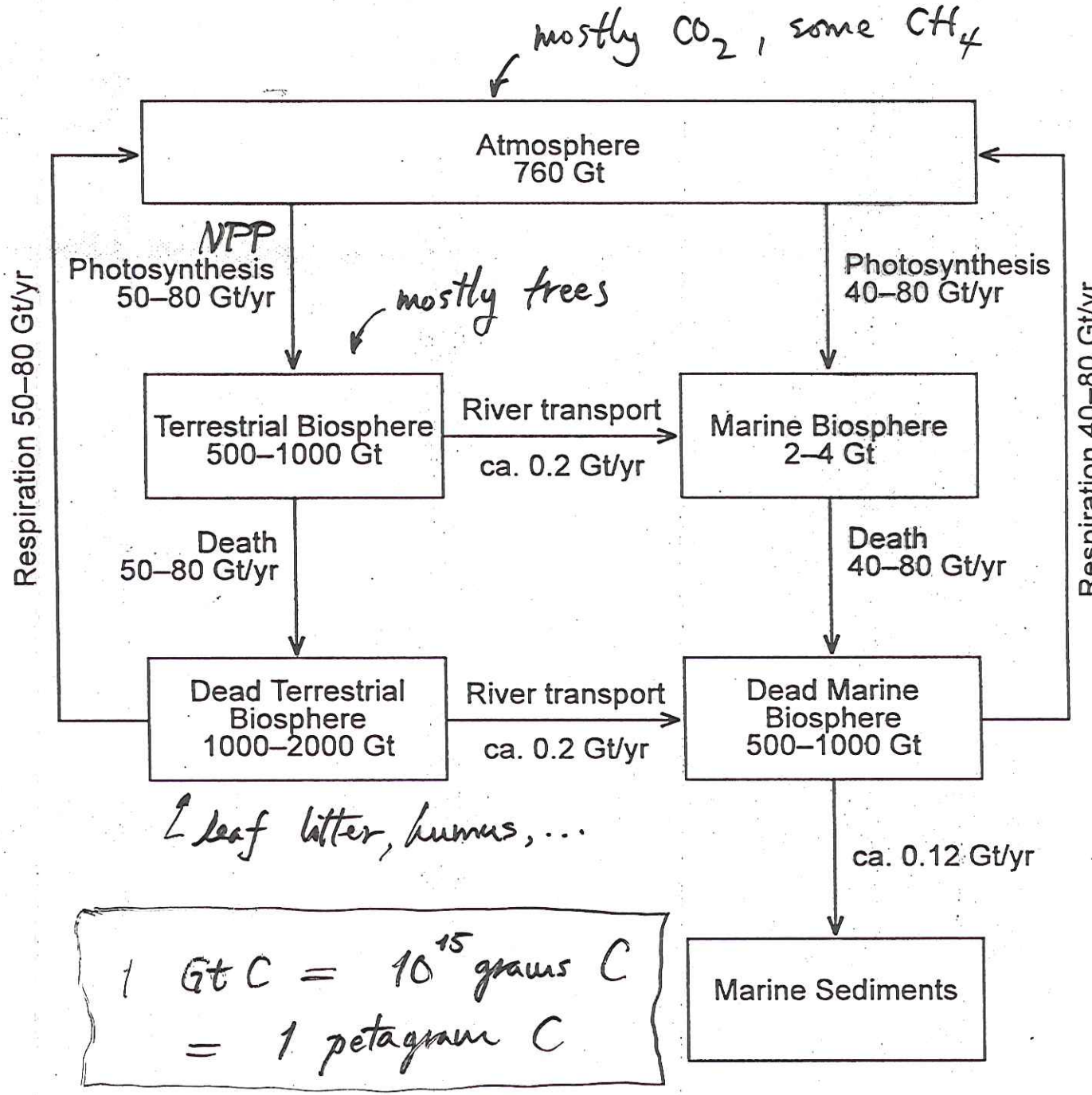

Steady-state box model for carbon

Figure 5.4. The biological parts of the carbon cycle. The carbon content of the several reservoirs is in Gt carbon (1 Gt = 10^{15} gm C). (Data from the compilation of Sundquist 1985)

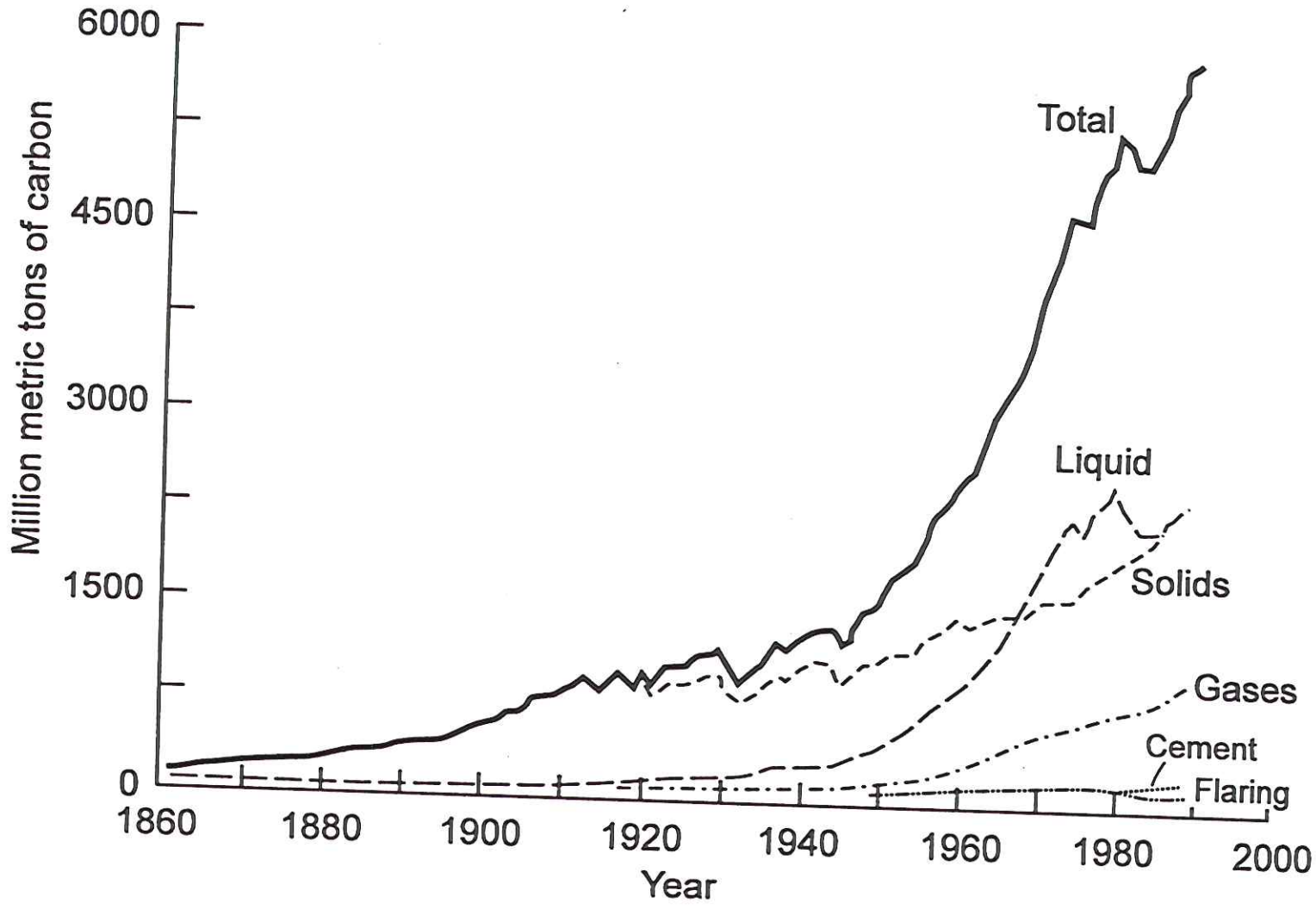

Figure 11.18. Global CO_2 emissions from fossil fuel burning and cement manufacture, 1860–1989. (From *Trends '91: A Compendium of Data on Global Change*)

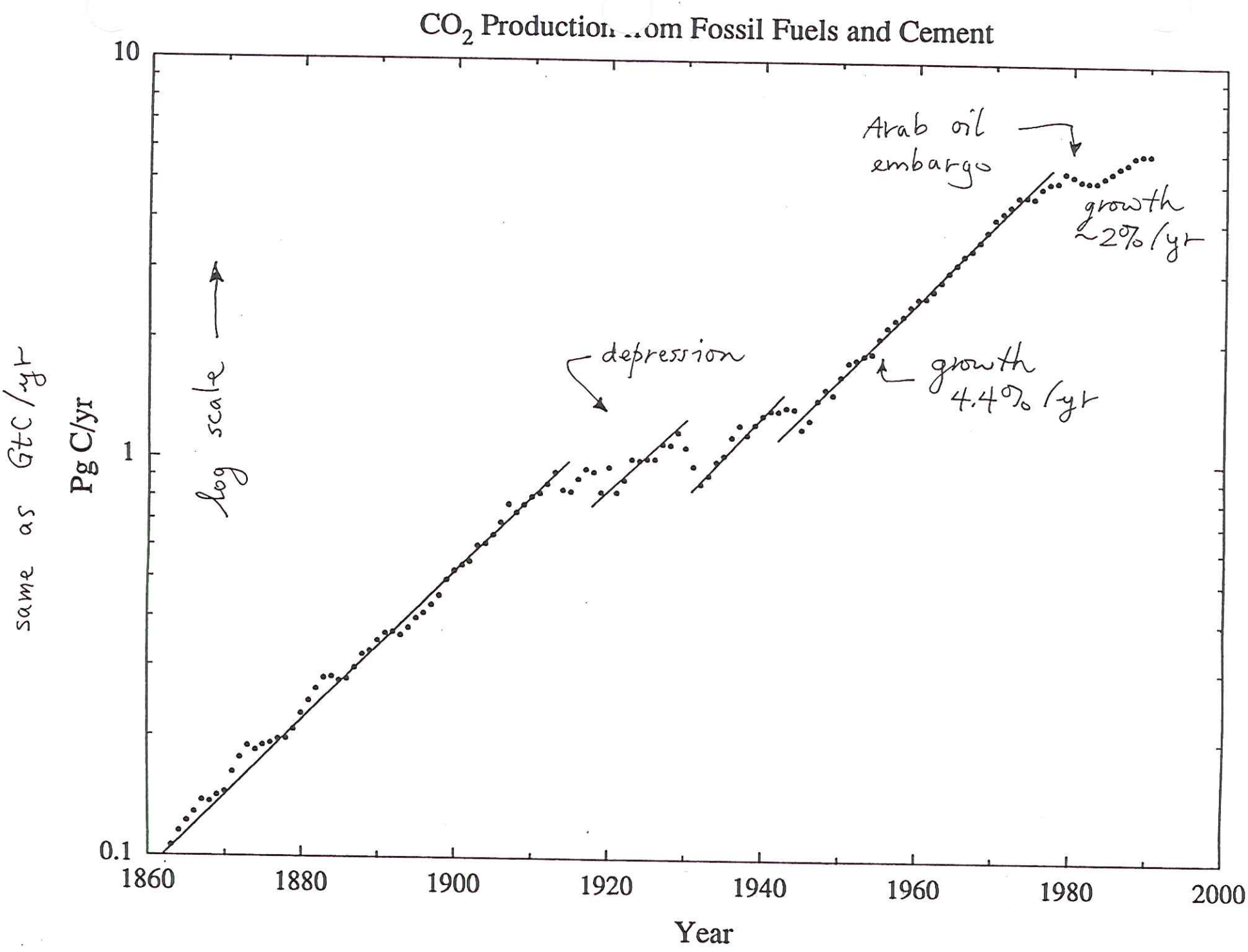
CO_2 Production ..om Fossil Fuels and Cement
10
1
0.1
Pg C/yr
same as GtC/yr
log scale
Arab oil embargo
growth ~2%/yr
depression
growth 4.4%/yr
1860
1880
1900
1920
1940
1960
1980
2000
Year

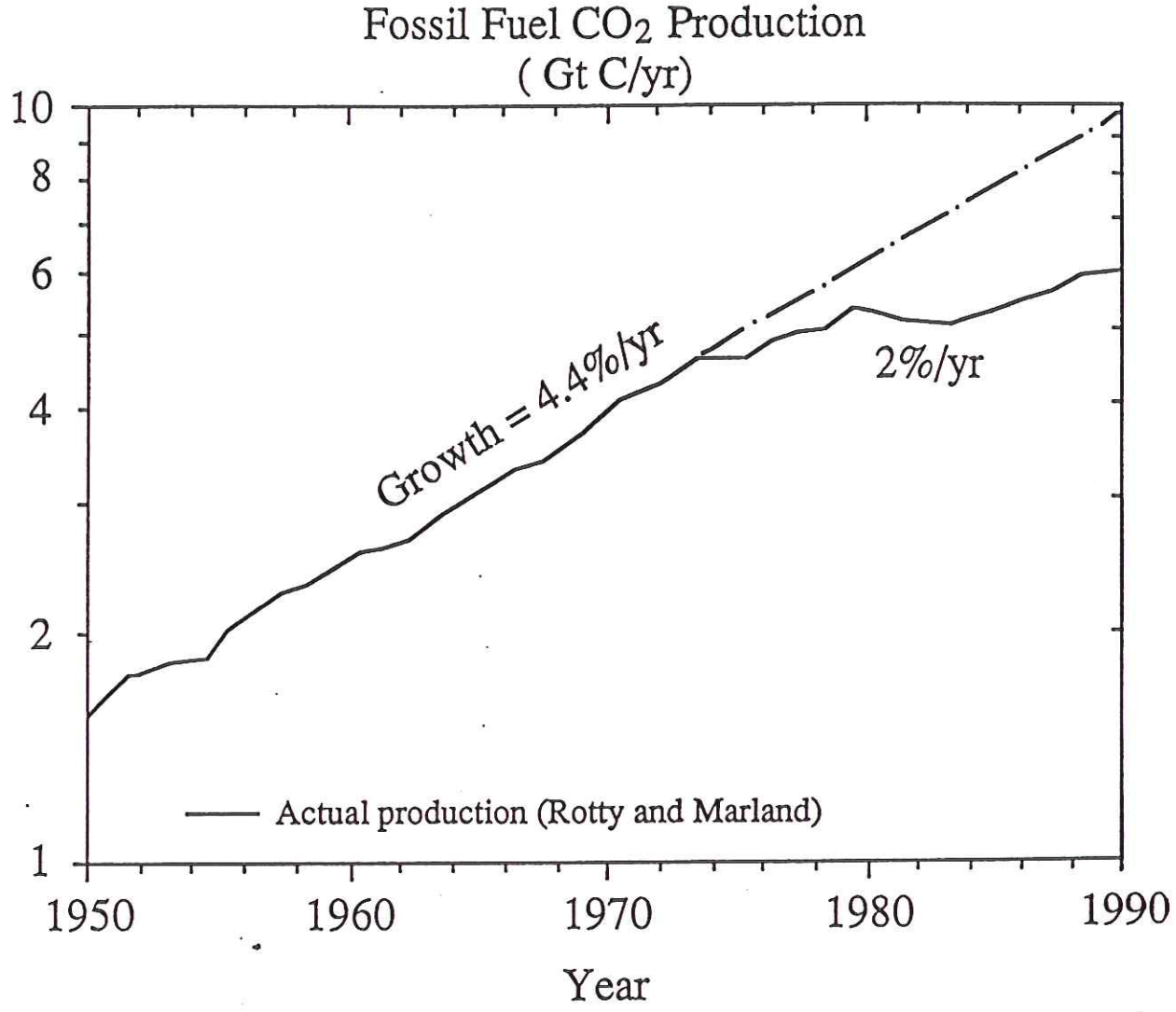
Fossil Fuel CO_2 Production
(Gt C/yr)
10
8
6
4
2
1
1950
1960
1970
1980
1990
Year
Growth = 4.4%/yr
2%/yr
Actual production (Rotty and Marland)

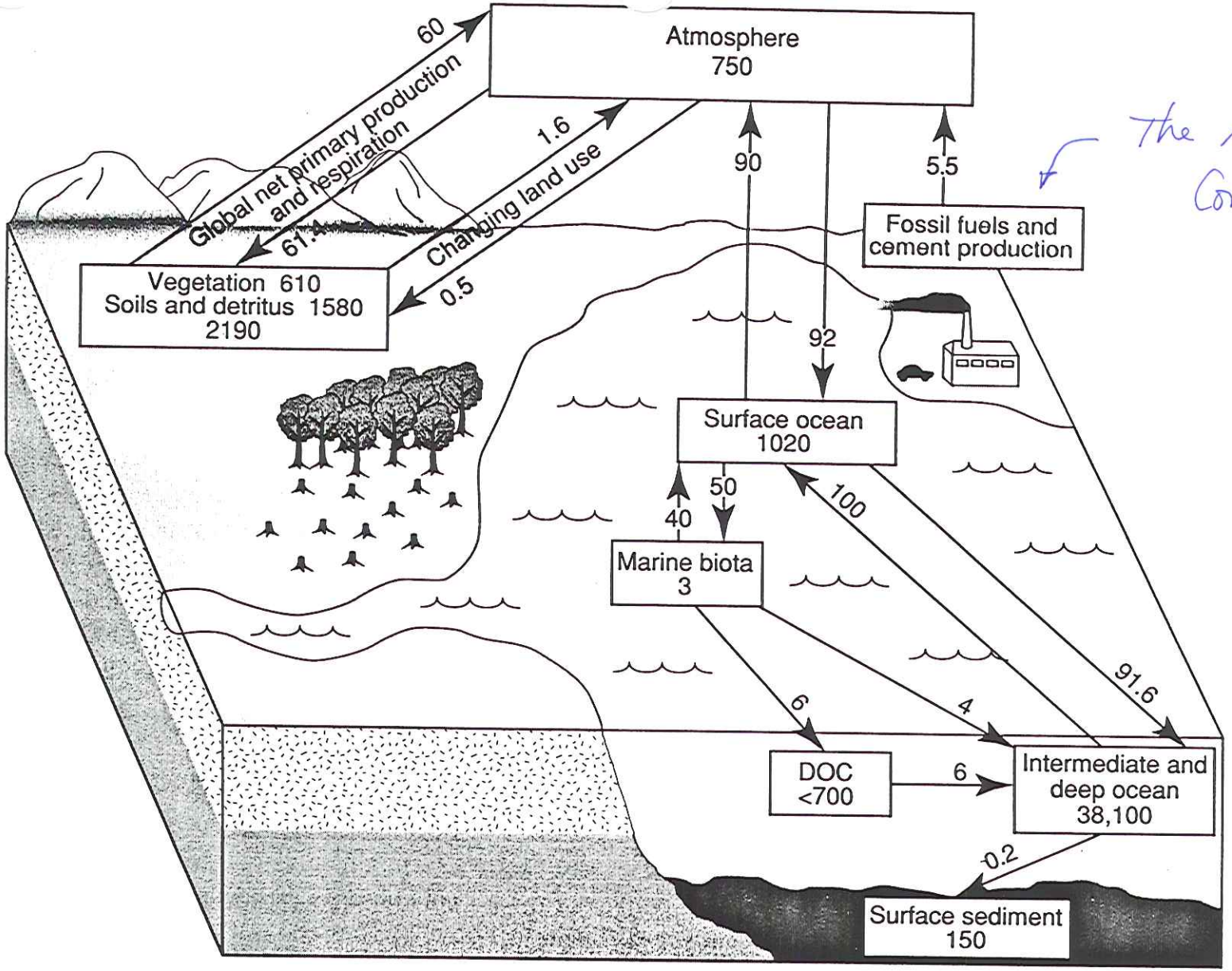

The Anthropogenic Contribution

Figure 4: The global carbon cycle. The numbers in boxes indicate the size in GtC of each reservoir. On each arrow is indicated the magnitude of the flux in GtC/yr (DOC = dissolved organic carbon).

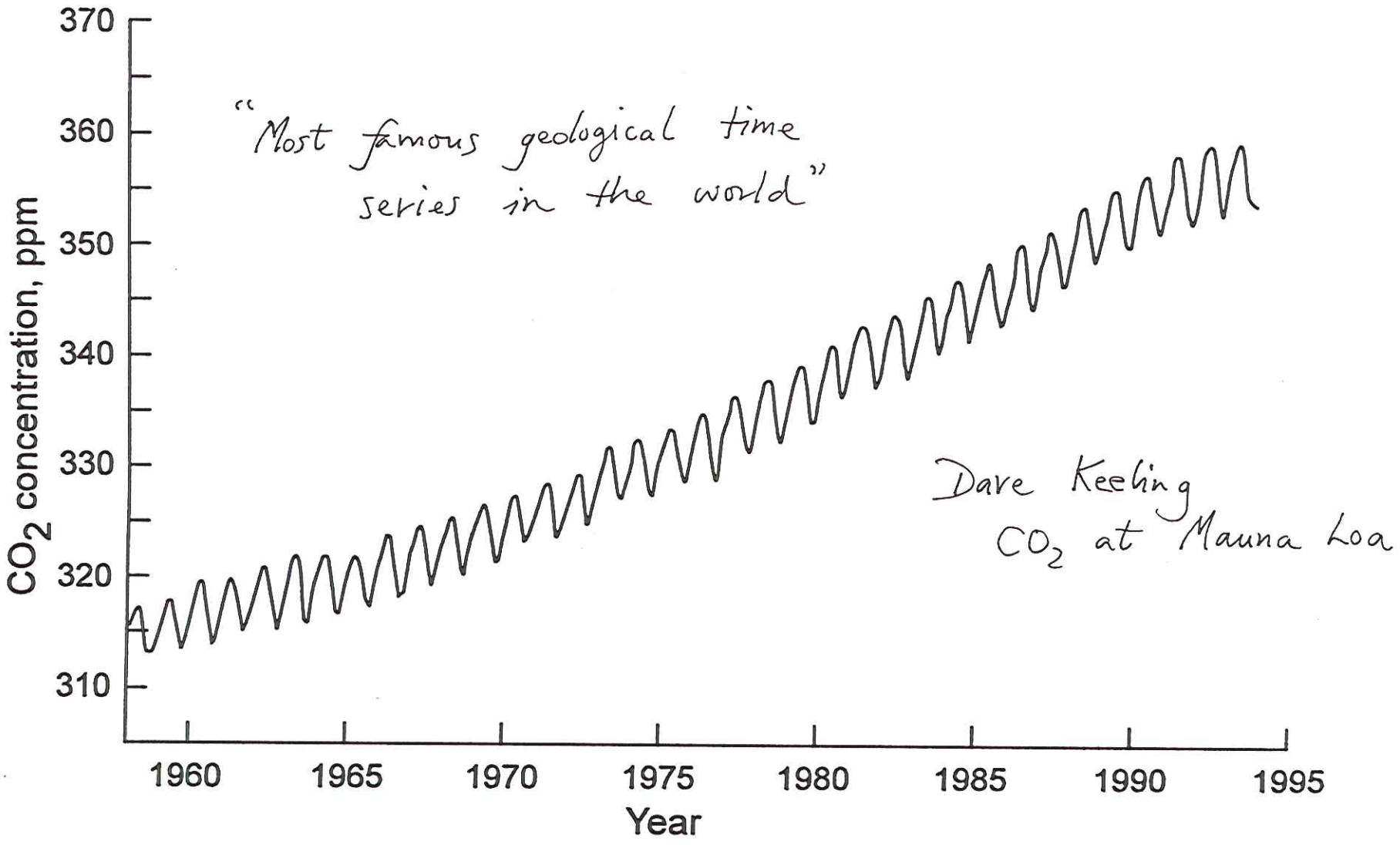
"Most famous geological time series in the world"
Dave Keeling
CO_2 at Mauna Loa
CO_2 concentration, ppm
370
360
350
340
330
320
310
1960
1965
1970
1975
1980
1985
1990
1995
Year

Secular increase of atmospheric CO_2 is global

1.5 ppm/yr or 0.42 %/yr

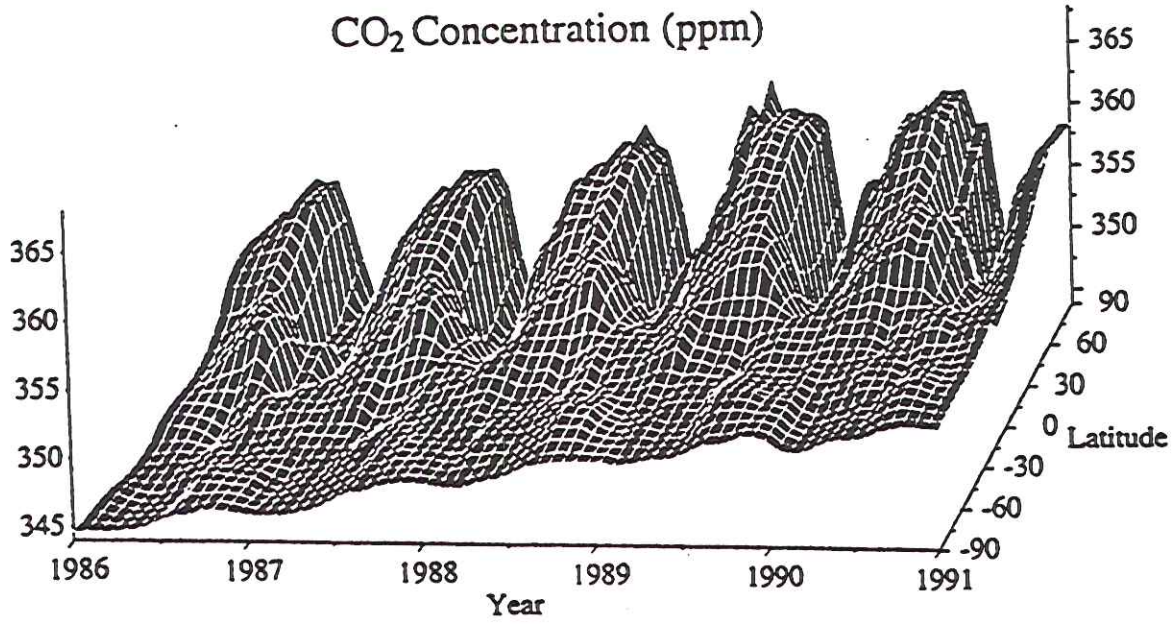

Fig. 9. Smoothed atmospheric CO_2 data as measured by the National Oceanic and Atmospheric Administration, Climate Monitoring and Diagnostics Laboratory's Flask Sampling Program (Conway et al. 1991).

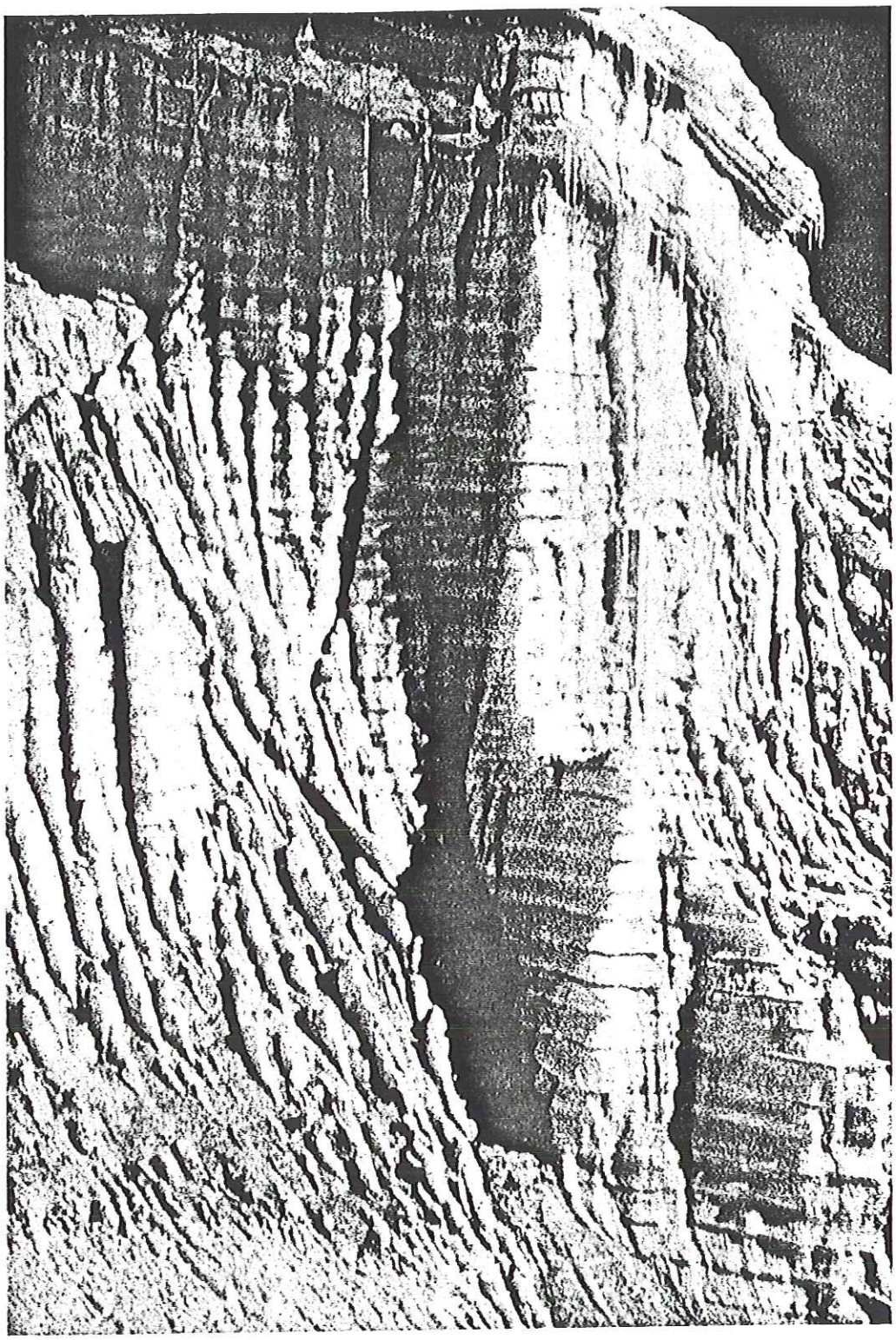

FIGURE 2–2 Quelccaya ice cap is located in the southern Peruvian Andes at an elevation of 5670 meters. This 50-meter ice cliff at the margin of the ice cap, photographed in 1983, has disappeared as of August 1995 as the result of increasing temperature (discussed in Chapter 6). This ice cap has annual layers (about 0.75 meters each) dating back 1500 years. (Photograph courtesy of Lonnie G. Thompson, Department of Geological Science and Byrd Polar Research Center of The Ohio State University.)

Figure 1.3 An ice core from the Antarctic glacier. The regions of annual surface thawing and recrystallization are clearly visible. (Courtesy of Robert Delmas, CNRS, France.)

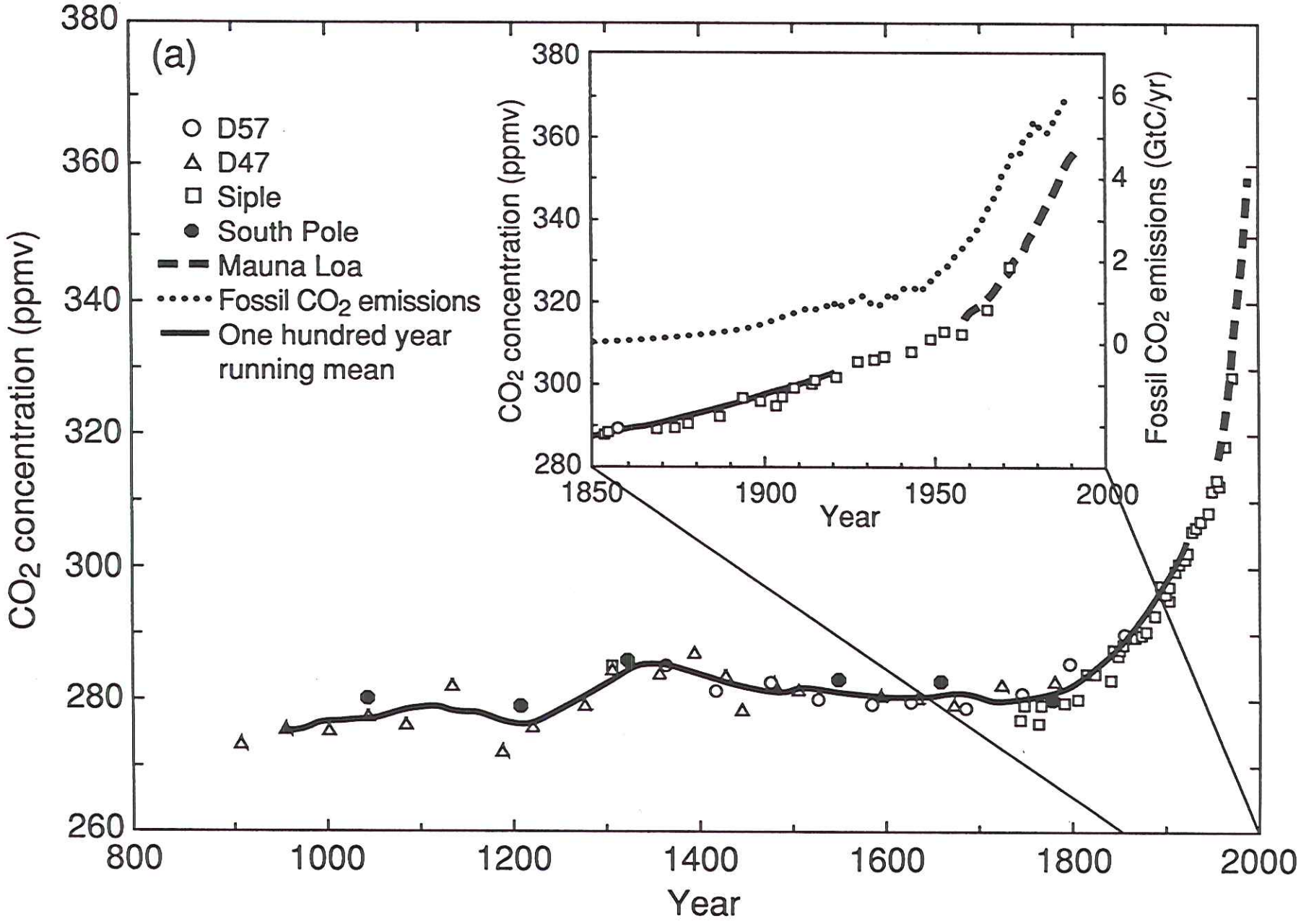
(a)
D57
D47
Siple
South Pole
Mauna Loa
Fossil CO_2 emissions
One hundred year running mean
CO_2 concentration (ppmv)
Year
380
360
340
320
300
280
260
800
1000
1200
1400
1600
1800
2000
CO_2 concentration (ppmv)
Fossil CO_2 emissions (GtC/yr)
Year
1850
1900
1950
2000
6
4
2
0

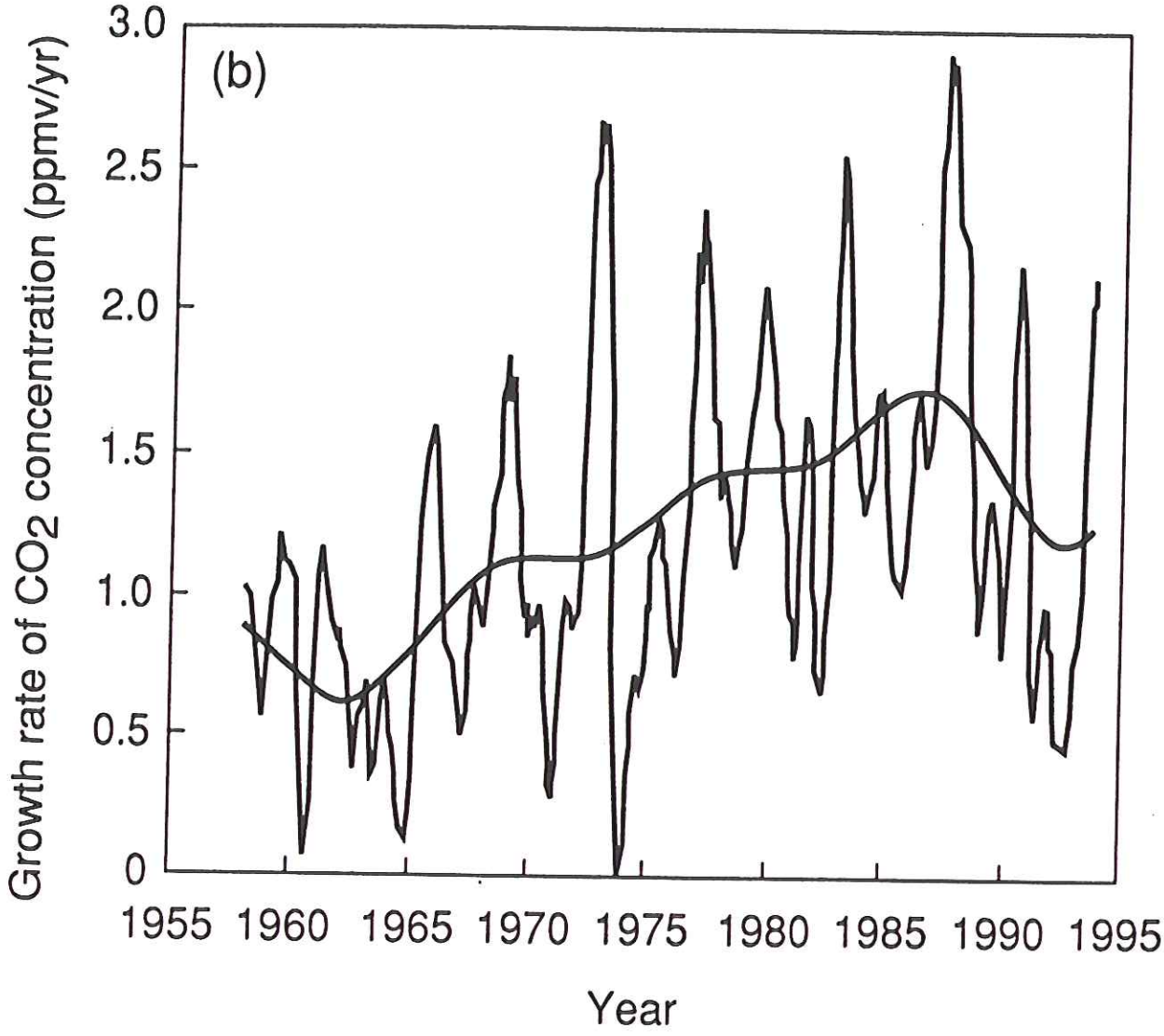

Atmospheric CO_2 growth rate 1.5 ppm/yr
or 0.42 %/yr

(0.0042)(760 GtC in atmosphere) = 3.2 GtC/yr

Anthropogenic emission rate is 5.5 GtC/yr

This is the "missing carbon" problem

Table 1: Annual average anthropogenic carbon budget for 1980 to 1989. CO_2 sources, sinks and storage in the atmosphere are expressed in GtC/yr.

CO_2 sources	
(1) Emissions from fossil fuel and cement production	5.5 ± 0.5
(2) Net emissions from changes in tropical land-use ← deforestation	1.6 ± 1.0
(3) Total anthropogenic emissions = (1)+(2)	7.1 ± 1.1
Partitioning amongst reservoirs	
(4) Storage in the atmosphere	3.2 ± 0.2
(5) Ocean uptake	2.0 ± 0.8
(6) Uptake by Northern Hemisphere forest regrowth	0.5 ± 0.5
(7) Additional terrestrial sinks (CO_2 fertilisation, nitrogen fertilisation, climatic effects) = [(1)+(2)]-[(4)+(5)+(6)]	1.4 ± 1.5 ← the "missing carbon"

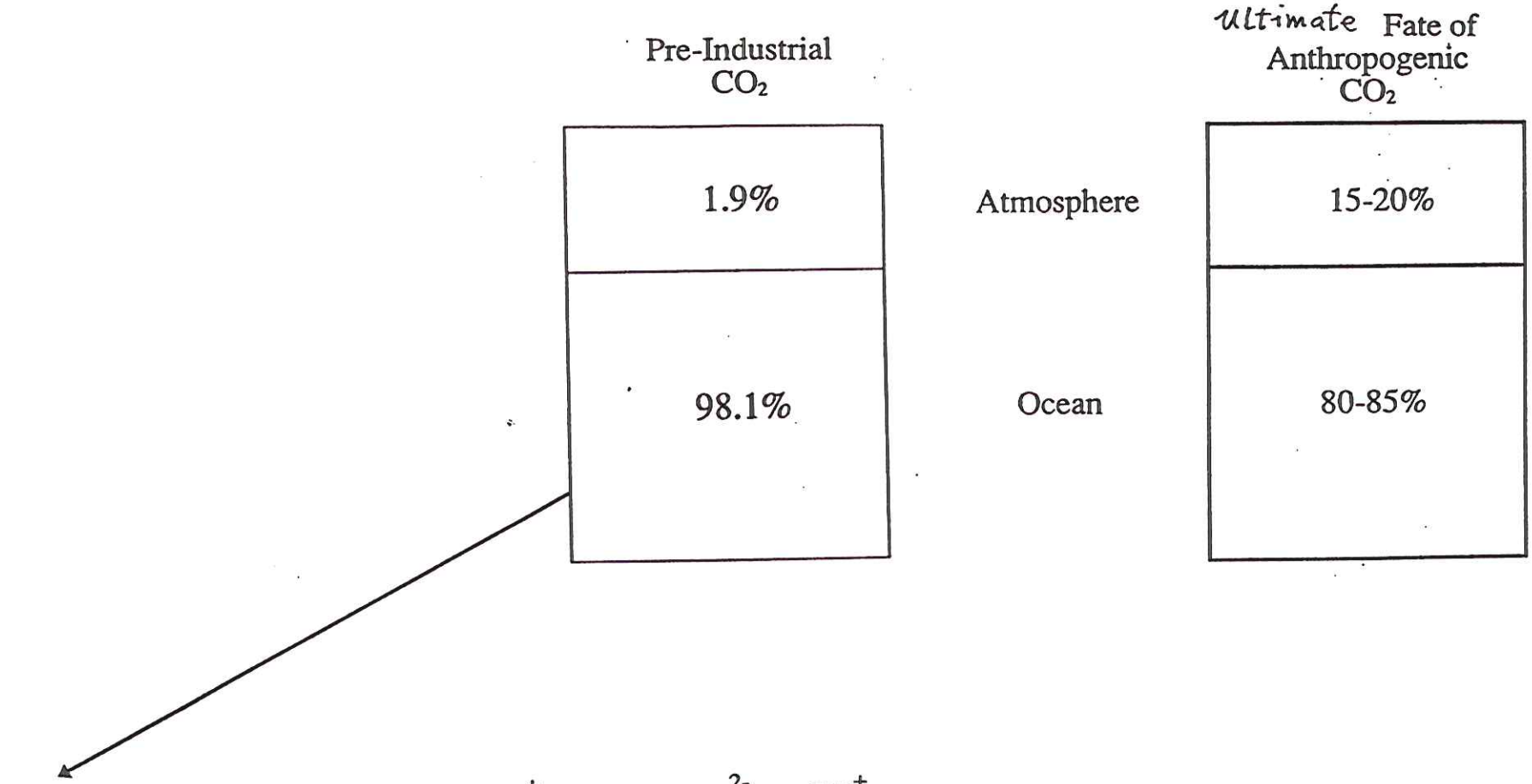
Pre-Industrial CO_2
Ultimate Fate of Anthropogenic CO_2
1.9%
Atmosphere
15-20%
98.1%
Ocean
80-85%
$CO_2 + H_2O \longleftrightarrow HCO_3^- + H^+ \longleftrightarrow CO_3^{2-} + 2H^+$
0.5%
88.9%
10.6%

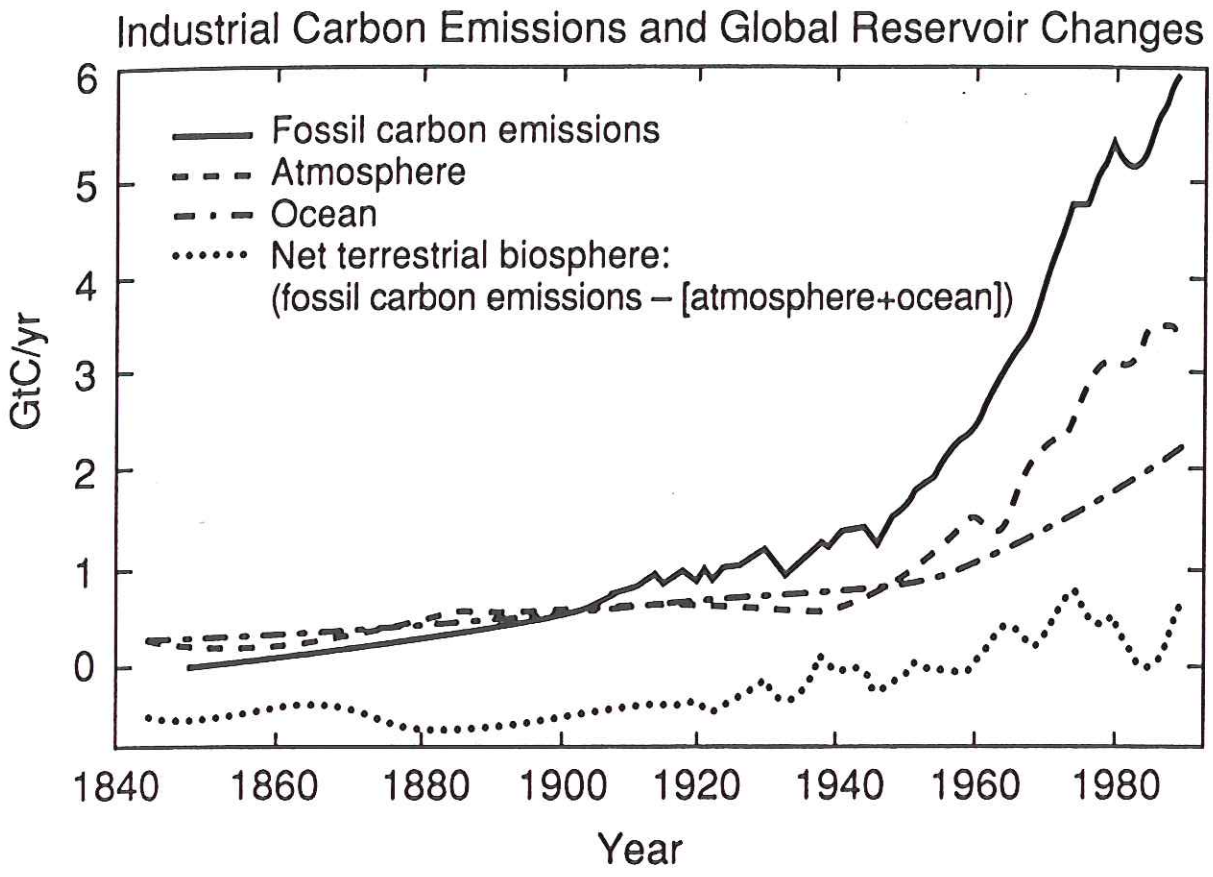

Figure 1.7: Fossil carbon emissions (based on statistics of fossil fuel and cement production), and representative calculations of global reservoir changes: atmosphere (deduced from direct observations and ice core measurements), ocean (calculated with the GFDL ocean carbon model), and net terrestrial biosphere (calculated as remaining imbalance). The calculation implies that the terrestrial biosphere represented a net source to the atmosphere prior to 1940 (negative values) and a net sink since about 1960.

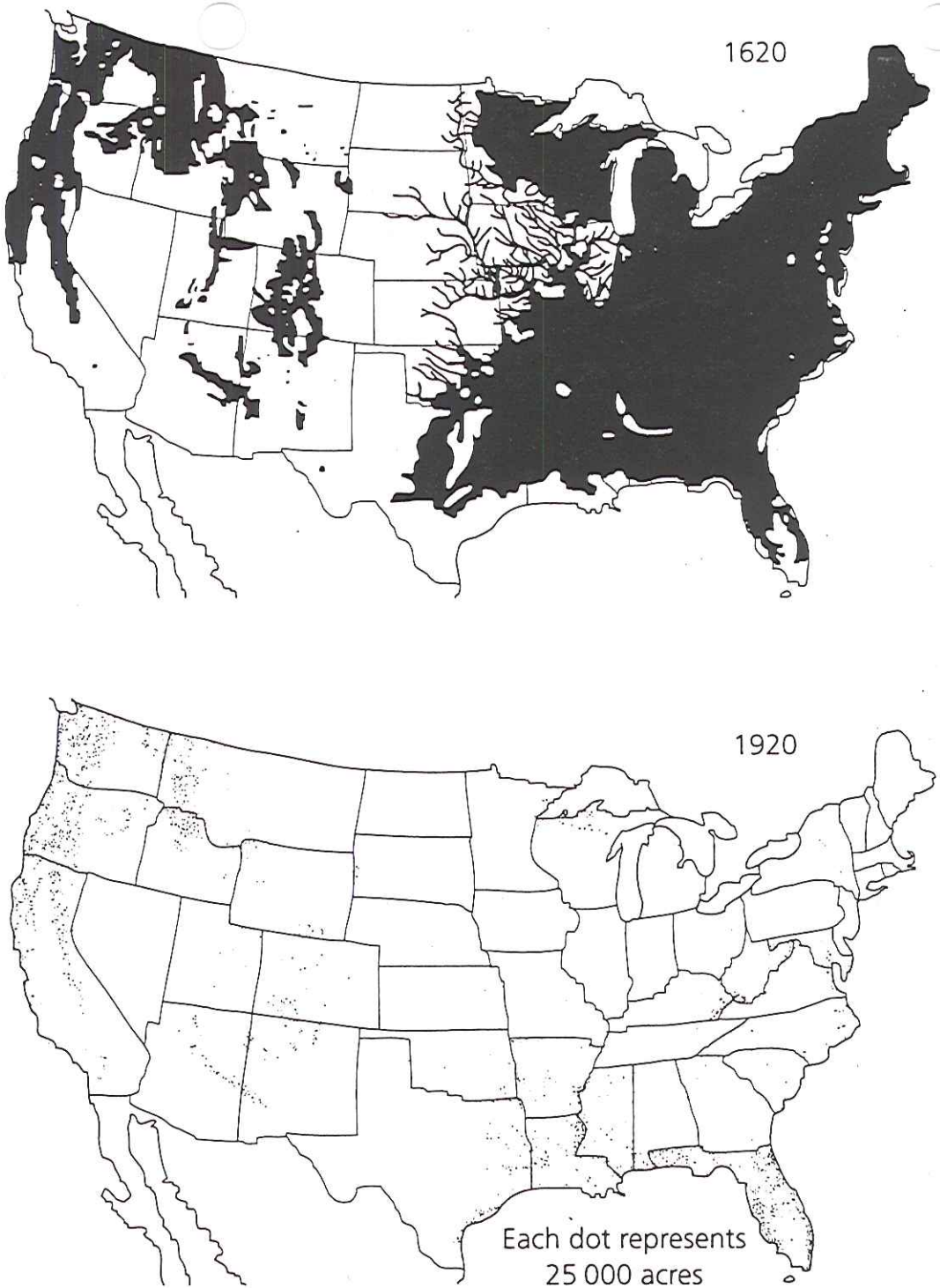

Loss of forest due to human colonization of North America between 1620 and 1920. After Goudie (1993) [47].

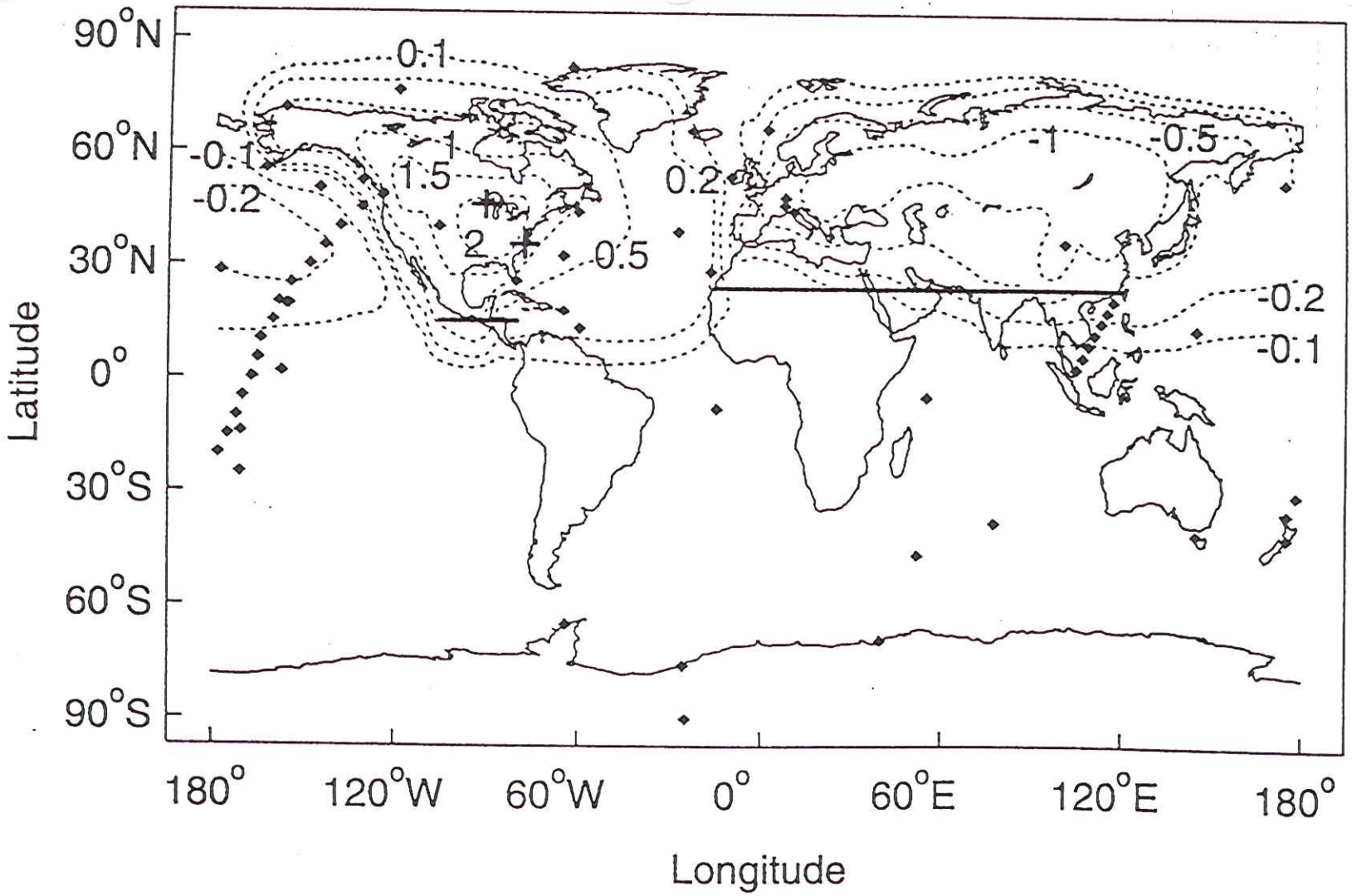

Fig. 1. A map of the atmospheric CO_2 sampling network. Sites are shown as solid diamonds. (The Globalview labels for the Northern Hemisphere stations are given in the legend of Fig. 3). The tall tower sites are shown as crosses. The thick horizontal lines divide the land surfaces into three regions where terrestrial carbon uptake has been estimated: North America, Eurasia–North Africa, and Tropics and Southern Hemisphere. The dotted contour lines show the difference between predicted surface CO_2 concentrations (ppm) with estimated terrestrial uptake and with North American terrestrial uptake set to zero (model results are shown for GCTM with the T97 sea-air fluxes).

Table 2. Estimated terrestrial carbon uptake for 1988 to 1992. Positive terrestrial carbon uptake is a flux out of the atmosphere. GCTM and SKYHI are the two atmospheric GCM models and T97 and OBM are the two air-sea flux estimates used in the inversions (see text).

Source region	Terrestrial uptake (Pg C year^{-1})				SD of the estimate* (Pg C year^{-1})	Mean and summary SE† (Pg C year^{-1})	Forest area (10^9 ha)
	GCTM		SKYHI				
	T97	OBM	T97	OBM			
			Three-region inversion				
North America	1.6	1.7	1.7	1.7	±0.5	1.7 ± 0.5	0.8
Eurasia and North Africa	0.5	0.5	−0.4	−0.2	±0.5	0.1 ± 0.7	1.2
Tropics and Southern Hemisphere	0.1	−1.1	0.9	−0.5	±0.1	−0.2 ± 0.9	2.1
Total	2.2	1.1	2.2	1.1	–	–	–
			Four-region inversion				
North America							
Boreal	0.4	−0.1	0.5	0.1	±0.3	0.2 ± 0.4	0.4
Temperate	1.2	1.7	1.2	1.3	±0.4	1.4 ± 0.5	0.4
Eurasia and North Africa	0.6	0.7	−0.4	0.0	±0.5	0.2 ± 0.7	1.2
Tropics and Southern Hemisphere	0.0	−1.3	0.9	−0.4	±0.1	−0.2 ± 0.9	2.1
Total	2.2	1.1	2.2	1.1	–	–	–

*The SD of the estimate was found by assuming that the Gaussian variance equals χ^2/q (q = 63) (*10*), and that data errors from different stations are independent. SDs of estimates obtained with T97 include the sampling uncertainty for oceanic CO_2 exchange (*15*), but those obtained with OBM include no oceanic uncertainty. However, the contribution of T97 error to the total uncertainty is small. †This is the mean of the estimates from the four combinations of atmospheric and oceanic models. The SE is $\sqrt{\sigma^2+V^2}$, where σ is the SD from the adjacent column and V is the SD of the four estimates in the first four columns.

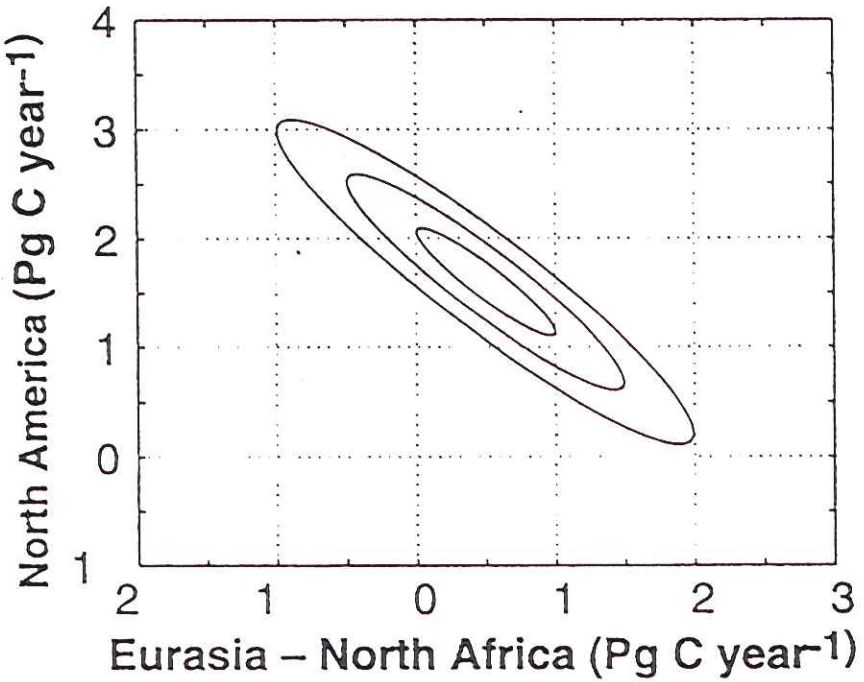

Fig. 2. Inversion uncertainties for North American terrestrial uptake versus Eurasia–North African terrestrial uptake. Ellipses of 1, 2, and 3 SDs are shown.

Table 1. Effect of various anthropogenic gases on the radiative balance of air. Middle column: efficiency of radiative forcing, expressed as a function of absorption per added molecule, with $CO_2 = 1$. Right-hand column: changes in radiative forcing between 1765 and 1990 due to increasing concentrations (Shine et al. 1990). The methane forcing change also includes the indirect effect due to formation of water vapor in the stratosphere

Gas	Normalized forcing per added molecule	Forcing change 1765–1990 ($W\,m^{-2}$)
CO_2	1	1.50
CH_4	21	0.56
N_2O	206	0.10
CFC-11	12 400	0.062
CFC-12	15 800	0.14
Other CFCs		0.085
		2.45

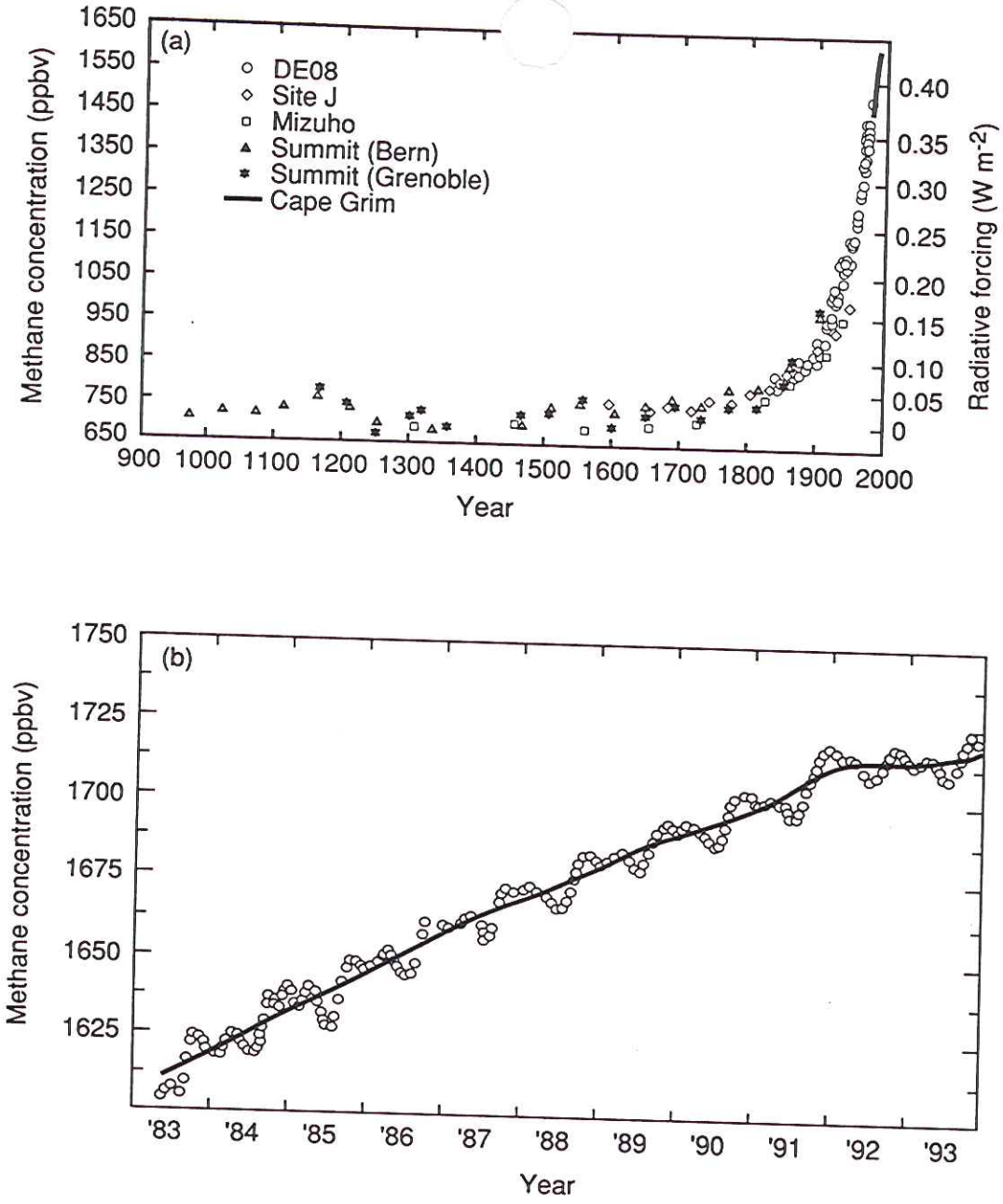

Figure 9: (a) CH_4 concentration derived from Antarctic ice cores over the past 1000 years. Direct observations of CH_4 concentration from Cape Grim, Tasmania, are included to demonstrate the smooth transition from ice core to atmospheric measurements. The radiative forcing resulting from increases in CH_4 relative to the pre-industrial period are indicated on the right-hand axis. The effect of overlap with N_2O is accounted for according to IPCC (1990). (b) Globally averaged CH_4 concentration for 1983 to 1993 showing the decline in growth rate during 1992 and 1993.

SOUTH PACIFIC

NEW ZEALAND: GAS TAX Farmers reacted angrily to a government proposal to tax the flatulence emitted by their cattle and sheep in an effort to reduce the nation's contribution to global warming. Last year New Zealand signed the Kyoto Protocol, agreeing to reduce greenhouse gases. Livestock emissions of methane and nitrous oxide, caused by the complex process of digesting grass, account for more than half the country's greenhouse gases, and the government wants the tax to help pay for research on the emissions. It would cost the average farmer up to $300 a year. Tom Lambie, the president of Federated Farmers, told The New Zealand Herald that the tax was unfair. "As far as I'm aware, we're the only country in the world to impose a levy like this," he said. *(Reuters)*

World Business Briefing, Page B2

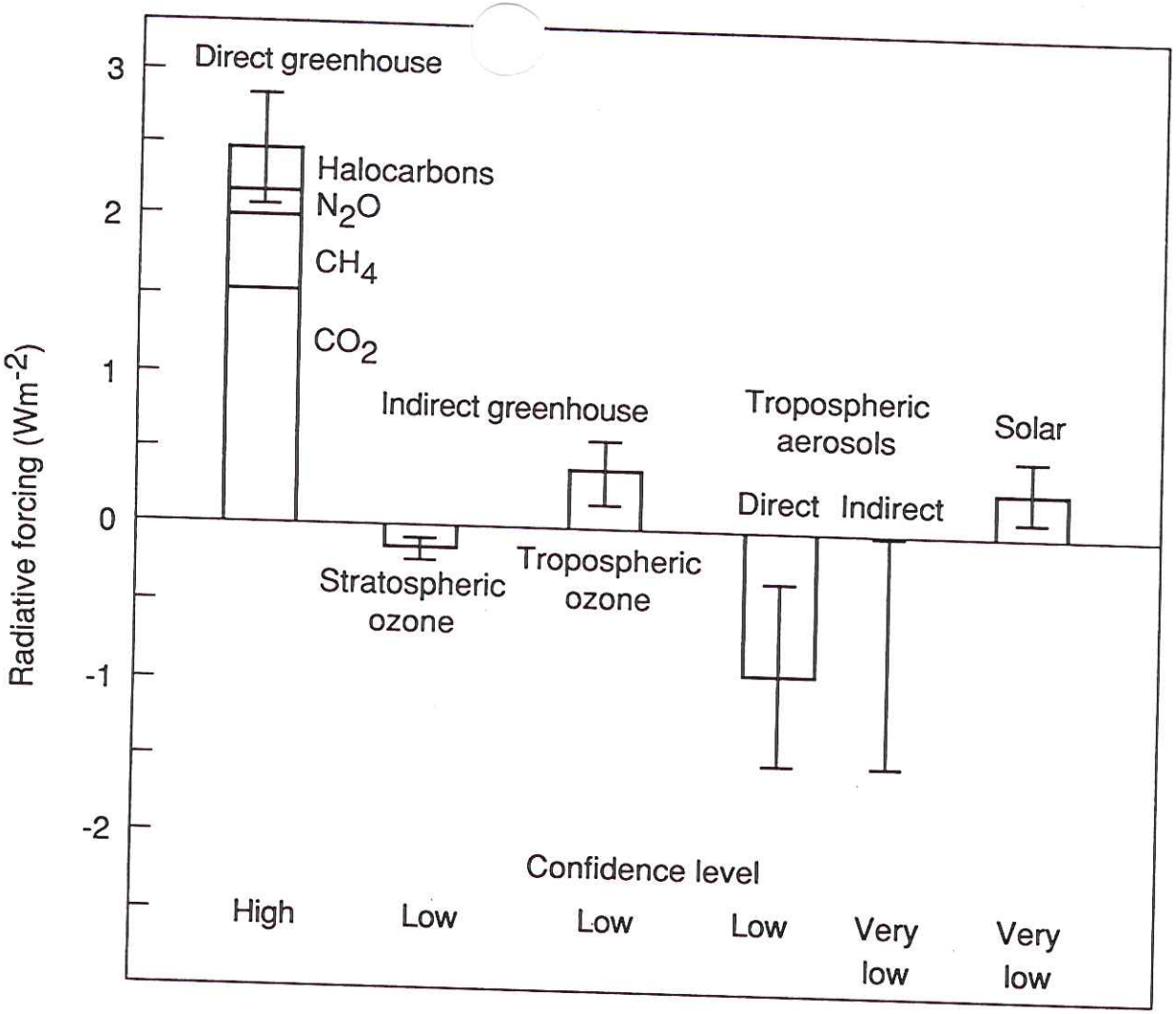

Figure 3: Estimates of the globally averaged radiative forcing due to changes in greenhouse gases and aerosols from pre-industrial times to the present day and changes in solar variability from 1850 to the present day. The height of the bar indicates a mid-range estimate of the forcing whilst the lines show the possible range of values. An indication of relative confidence in the estimates is given below each bar. The contributions of individual greenhouse gases are indicated on the first bar for direct greenhouse gas forcing. The major indirect effects are a depletion of stratospheric ozone (caused by the CFCs and other halocarbons) and an increase in the concentration of tropospheric ozone. The negative values for aerosols should not necessarily be regarded as an offset against the greenhouse gas forcing because of doubts over the applicability of global mean radiative forcing in the case of non-homogeneously distributed species such as aerosols and ozone (see Section 1 and Section 7).

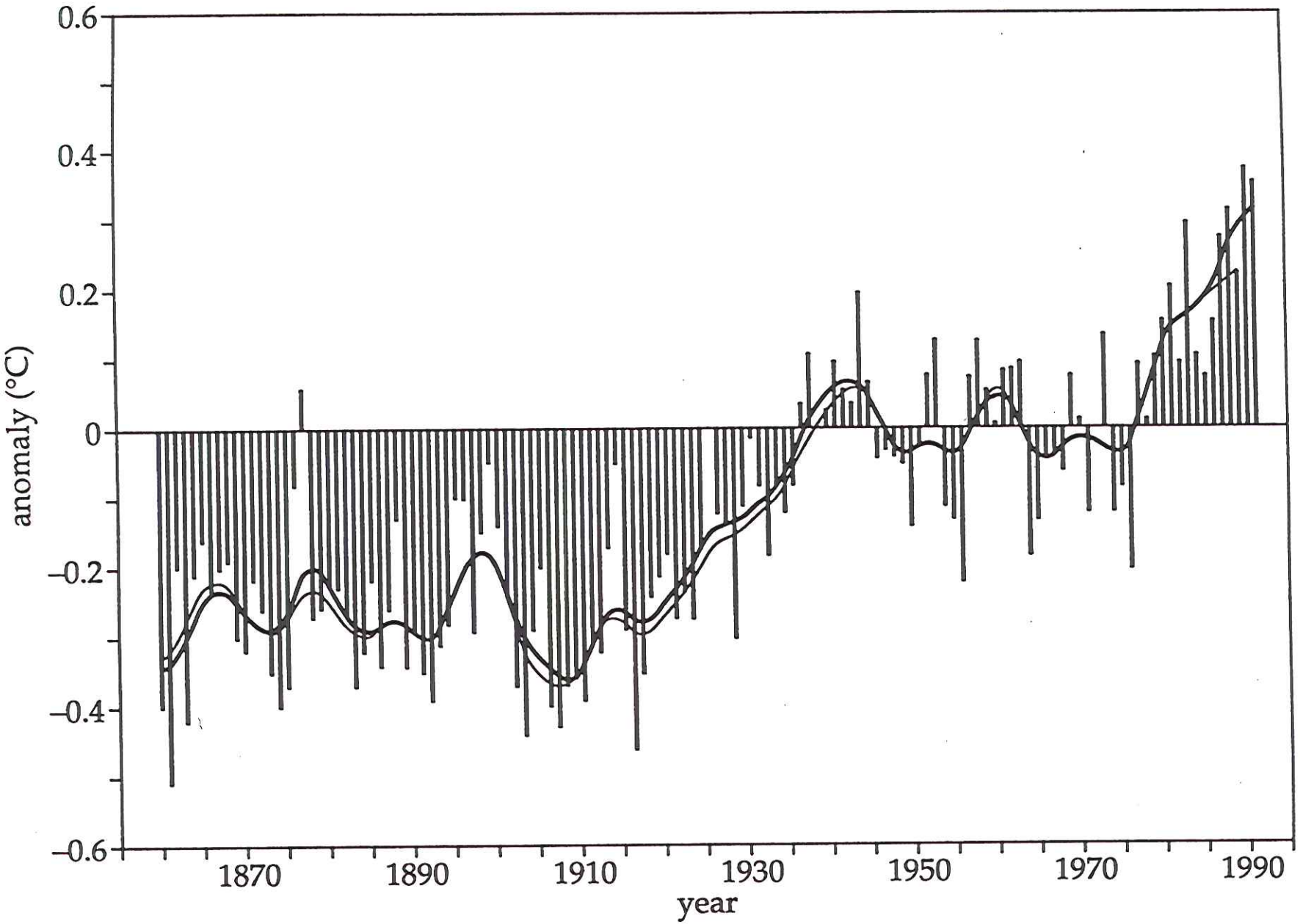

Figure 1.9 Combined land, air and sea surface temperature anomalies between 1861 and 1991, relative to the average temperature 1951–1980. (From IPCC 1992.)

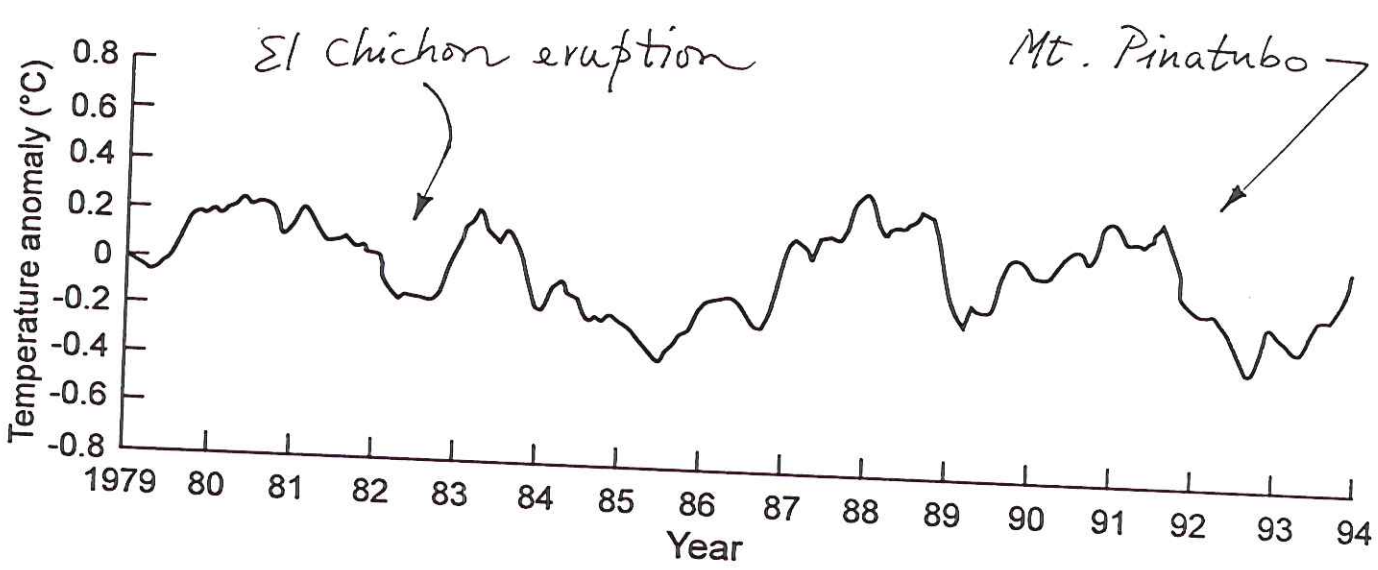

Figure 11.22. Mean global tropospheric temperature anomalies from satellite data (85°S–85°N) from 1979 to 1993. (Data from R. W. Spencer and J. R. Christy; Halpert et al. 1994; see also Kerr 1995)

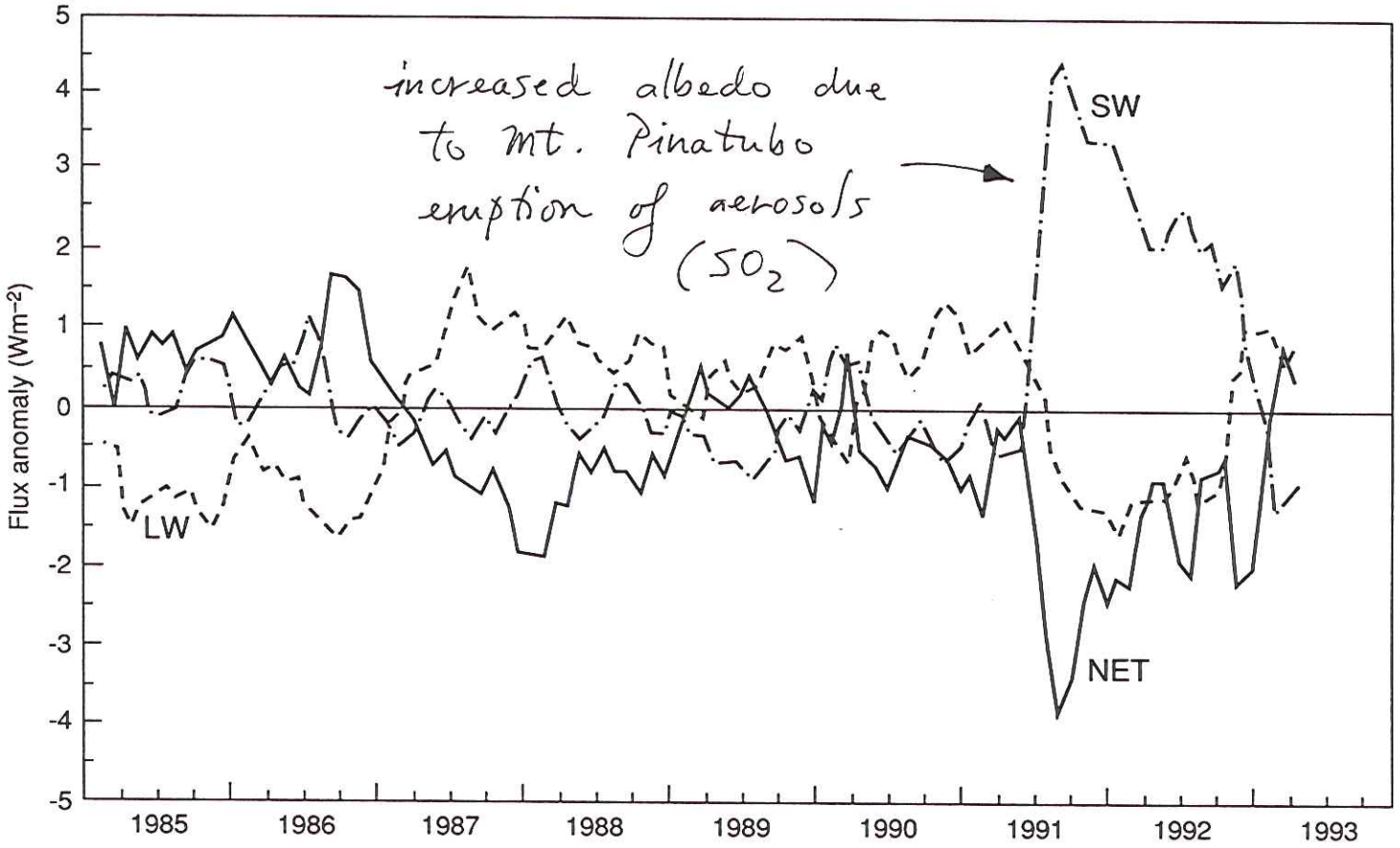

Figure 4.6: Time series of smoothed wide field of view Earth Radiation Budget Experiment long-wave (LW), short-wave (SW) and net (LW-SW) irradiance anomalies (in Wm^{-2}) between 40°N and 40°S relative to the 5 year (1985-1989) monthly mean (after Minnis *et al.*, 1993, updated by Minnis, 1994). The deviation starting in mid-1991 is mainly due to the Mt. Pinatubo eruption – the net anomaly in August (about -4 Wm^{-2}) is almost three times higher than the standard deviation computed between 1985 and 1989.

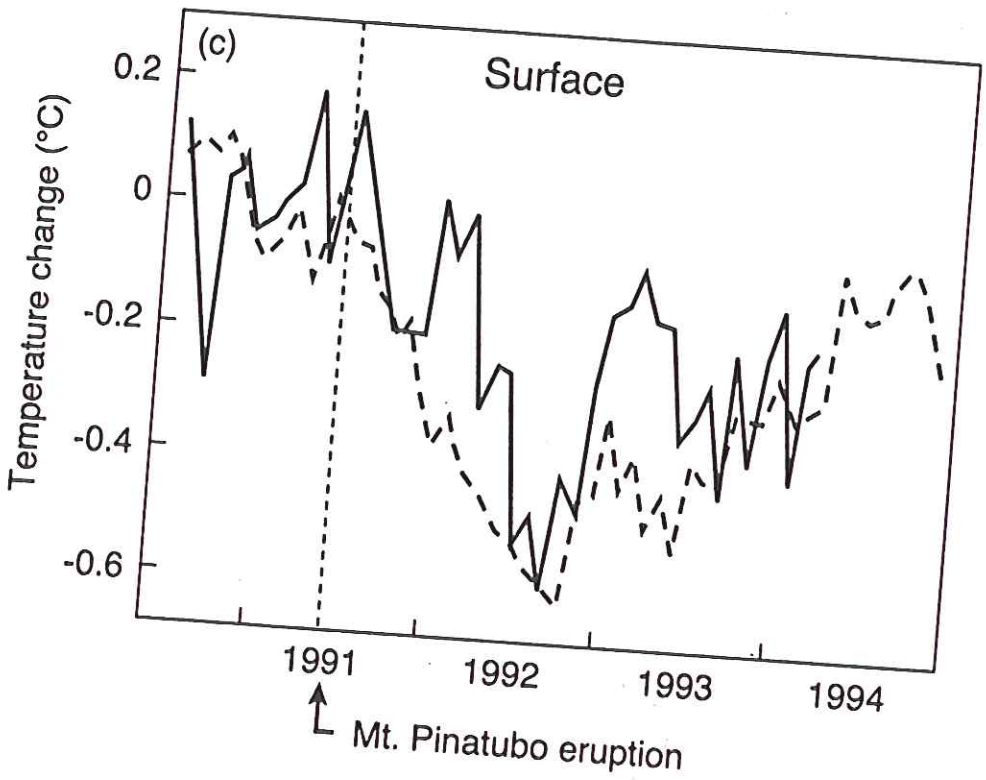

Figure 4.7: Observed and modelled (from the GISS GCM) monthly mean temperature changes over the period of the Mt. Pinatubo eruption (updated from Hansen *et al.*, 1993a). The eruption is indicated by the vertical dashed line. (a) Stratospheric temperatures are from satellite observations and show the 30 mb zonal mean temperature at 10°S and are supplied by M.Gelman, NOAA; the model results are the 10-70 mb layer at 8 to 16°S. The zero is the mean for 1978 to1992. (b) Tropospheric temperatures are from satellite observations and are supplied by J. Christy, Univ of Alabama; the observations and model results are essentially global. The zero is given by the mean for the 12 months preceding the eruption. (c) Surface temperatures are derived from meteorological stations; the observations and model results are essentially global. The zero is given by the mean for the 12 months preceding the eruption. Note that the model results use a simple prediction of the way the optical thickness of the volcanic cloud varied with time, made soon after the eruption, rather than detailed observations of the evolution of the cloud.

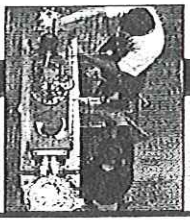

CLIMATE CHANGE

Possibly Vast Greenhouse Gas Sponge Ignites Controversy

As greenhouse warming experts try to predict how much the world's climate may heat up in the next century, they keep bumping up against a mystery: Where does much of the carbon dioxide (CO_2) pumped into the air actually end up? Answering this question could have huge ramifications for nations that ratify the climate change treaty signed in Kyoto, Japan, last December: Countries shown to harbor substantial carbon "sinks" could argue that an ability to soak up excess CO_2 should offset their emissions.

If those arguments prevail, it appears that North America may have drawn the winning ticket in the carbon sink sweepstakes. In what is shaping up as one of the most controversial findings yet to emerge in the greenhouse gas debate, a team of researchers on page 442 of this issue of *Science* presents evidence that North America sops up a whopping 1.7 petagrams of carbon a year—enough to suck up every ton of carbon discharged annually by fossil fuel burning in Canada and the United States. The magnitude of the apparent sink, says team member Jorge Sarmiento of Princeton University, "is going to be a lightning rod for all sorts of criticism."

Indeed, critics have already thrown up a fistful of red flags, attacking the study for everything from its methodology to its implications. "There's a huge amount of skepticism about the result," says ecologist David Schimel of the National Center for Atmospheric Research in Boulder, Colorado, who notes that at least one other group has calculated a much smaller North American sink. Moreover, a second paper in this issue—by a group led by Oliver Phillips of the University of Leeds in the United Kingdom (p. 439)—adds to the uncertainty. It points to a carbon sink in tropical South America so large that it is hard to reconcile with the Sarmiento group's results.

Especially worrisome, Schimel and others say, is that groups opposed to the Kyoto treaty will seize on the estimate to argue that the United States doesn't need to reduce its emissions to comply with the accord. "We're all really concerned that many people will find it convenient to accept the result," Schimel says. At the same time, scientists say this sort of calculation is a key step toward honing our understanding of the global carbon cycle. "The authors deserve a lot of credit for sticking their necks out," says climate modeler Inez Fung of the University of California, Berkeley.

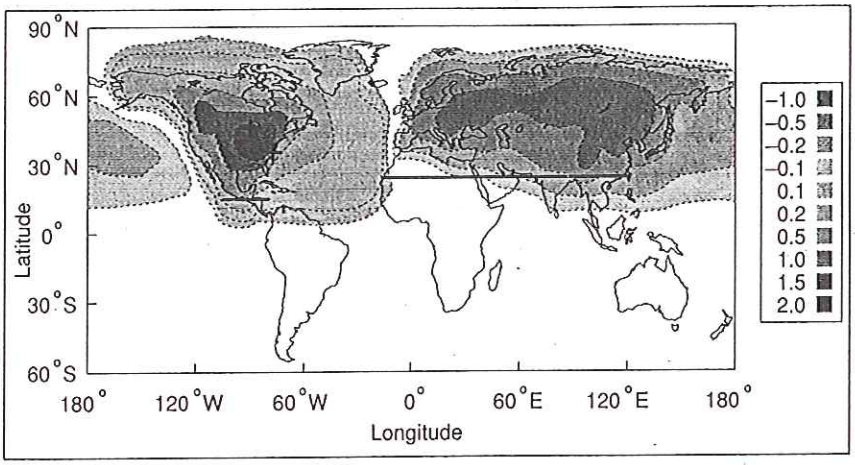

Disappearing act. Contours show how predicted CO_2 levels (in parts per million) would change if there were no terrestrial uptake in North America. Measured levels decline, rather than increase, from west to east North America, however, implying a large carbon sink.

At the heart of the debate is a simple math problem, resembling a chronic inability to balance one's checkbook, that has bedeviled scientists for nearly 2 decades. The balance sheet looks like this: Less than half of the 7.1 petagrams of carbon produced by human activity each year stays in the atmosphere. Although about 2 petagrams go into the oceans, another 1.1 to 2.2 petagrams appear to vanish into the land, likely taken up by plants during photosynthesis. Figuring out what's going on—whether the extra CO_2 is spurring faster tree growth, for example, or carbon is disappearing into soils—is crucial to learning whether reforestation and other actions might help stave off warming (*Science*, 24 July, p. 504). "If you understood the mechanism, you'd be in a much better position to say whether the sink will continue," says biogeochemist Richard Houghton of Woods Hole Research Center in Massachusetts.

To get at how much carbon the different land masses are absorbing, Sarmiento and his colleagues with the Carbon Modeling Consortium (CMC), based at Princeton, used an approach called inversion modeling. They first gathered data on atmospheric CO_2 levels taken from 1988 to 1992 at 63 ocean-sampling stations. Next, they divided the world into three regions—Eurasia, North America, and the rest—then fed the CO_2 data into two mathematical models: one that estimates how much carbon the oceans absorb and release, and another that gauges how CO_2 is spread across the globe by wind currents. When they fitted their models to the data, they found that, surprisingly, CO_2 levels dropped off slightly from west to east across North America—even though fossil fuel emissions should boost levels in the east. That meant there must be a big carbon sink in North America.

Straining belief among other experts is the sink's estimated magnitude—1.7 petagrams of carbon per year, plus or minus 0.5 petagrams—roughly equaling the continent's fossil fuel carbon emissions of 1.6 petagrams. "It's hard for me to know where that much carbon could be accumulating in North America," says Houghton. Data from forest inventories suggest the U.S. sink absorbs only 0.2 to 0.3 petagrams of carbon a year. Sarmiento's team suggests that the inventories have missed a lot of forest regrowth on abandoned farmland and formerly logged forests in the east fertilized by CO_2 or nitrogen pollution, and that they fail to account for carbon stored in soils and wetlands. But the result also suggests that Eurasia's immense forests are taking up only a fifth as much carbon as U.S. forests. "Ecologically, it seems al-

CREDIT: S. FAN ET AL.

most incomprehensible," Schimel says.

Several modelers contend that the study is riddled with uncertainties. For one thing, the two models used to gauge carbon flux "could easily be off by just a little bit, and you get a very different conclusion," says Fung. The results could also be skewed by a dearth of data from the North Atlantic, as the authors note in their paper. For example, the group threw out readings off Sable Island, Nova Scotia, because the data were unreliable, says team member Pieter Tans of the National Oceanic and Atmospheric Administration. Factoring in Sable Island, the sink shrinks by 30%.

Even if the results do hold up, observers note, the CMC study's time period includes the 1991 Mount Pinatubo eruption, which led to cooler, wetter conditions and a much higher global carbon uptake than usual. "Some of this sink must clearly be ... transient," says Martin Heimann, a modeler at the Max Planck Institute for Biogeochemistry in Jena, Germany. And the findings clash with those from a team led by Peter Rayner of Monash University in Australia, which calculates a North American sink of only 0.6 petagrams of carbon from 1988 to 1992—about one-third the CMC group's estimate. The Australian group's results will be published next year in *Tellus*.

The CMC team acknowledges that its results strain credibility. "I have trouble quite believing" the size of the sink, says Tans, adding that "We're pushing the data pretty far." But, says Sarmiento, "we've really carefully analyzed the data in a lot of different ways." U.S. Geological Survey geochemist Eric Sundquist agrees: "The paper is a credible and rigorous interpretation of the available data."

More and better data, including direct measurements of carbon storage and flux over land, will be needed to narrow the gap between the two studies. Already, this approach has turned up a big surprise: According to the U.K. group's results, undisturbed tropical forests in South America are getting thicker and may account for about 40% of the missing sink, a figure seemingly at odds with the CMC group's inversion results. The study is the first to pool data from measuring carbon storage, or biomass, over 2 decades at over 150 tropical forest plots worldwide. "This illustrates the types of studies that really need to be integrated," says Sundquist.

Before this research has time to mature, however, the possibly vast North American carbon sink could be the subject of heated debate in climate treaty implementation talks next month in Buenos Aires, Argentina. If the CMC team's findings are accurate, "the most obvious conclusion" would be that "there's no need for the U.S. and Canada to curb emissions," says Heimann. Indeed, Steven Crookshank of the American Petroleum Institute says the study "calls into question the scientific basis on which we're making these decisions, when we still don't know if the United States is even emitting any carbon in the net."

But some observers argue that a large North American sink should not be an excuse to go easy on emission controls. Maturing forests eventually stop storing carbon, so "this part of the missing sink [won't] be with us forever or even much longer," says atmospheric physicist Michael Oppenheimer of the Environmental Defense Fund in New York City. "The existence of the sink isn't important. What's important is the changes in the sink."

–JOCELYN KAISER

SOURCES: NATIONAL SCIENCE EDUCATION STANDARDS; CALIFORNIA ACADEMIC STANDARDS COMMISSION; PHOTO: VISUALS UNLIMITED

CREDIT: S. FAN *ET AL.*

SCIENCE EDUCATION

California Adopts Controversial Standards

Third-graders in California will be taught about the periodic table, and sixth-graders will learn about Earth's "lithospheric plates" under a new set of standards* approved last week by the state Board of Education. The standards—which will be used to revise the state curriculum, set guidelines for textbooks, and develop statewide tests—have been sharply attacked by many science education reformers, who contend that they focus too much on detailed knowledge and too little on concepts. Although the board's action appears to put an end to the controversy, critics are hoping that the winner of next month's gubernatorial race will revive the debate.

The standards reflect California's first attempt to spell out what students in kindergarten through 12th grade should learn about science. They follow on the heels of mathematics standards that were even more hotly contested before their adoption last December (*Science*, 29 August 1997, p. 1194). New tests for the state's 5.5 million students are scheduled to be ready in 2000—the same year public school textbooks will have to meet new guidelines. Those are expected to influence science teaching across the country, as California represents more than 10% of the national textbook market.

Last Friday's unanimous vote by the board came after a final flurry of lobbying and letter-writing by more than a dozen scientific societies (including the American Association for the Advancement of Science, which publishes *Science*). Some of these groups offered to help rewrite the final draft to bring it into line with National Science Education Standards issued in 1996 by the National Academy of Sciences (NAS). "It doesn't match the [national] standards in any way," says NAS President Bruce Alberts. He and others believe that the state standards contain so much factual material that teachers will be forced to skip more in-depth learning activities that would give students a better understanding of the scientific process.

But others praise the California standards as a challenging but realistic set of ex-

* See http://www.ca.gov/goldstandards; revisions are at http://www.cde.ca.gov/board/board.html

WHAT THE BATTLE'S ABOUT

NAS STANDARDS (Physical Science, grades K-4)

"Materials can exist in different states—solid, liquid, and gas. Some common materials, such as water, can be changed from one state to another by heating or cooling."

[Elements are introduced in grades 5-8; atoms are covered in grades 9-12.]

CALIFORNIA STANDARDS (Physical Science, grade 3)

"Matter has three forms: solid, liquid, and gas. ... Evaporation and melting are changes that occur when the objects are heated. ... All matter is made of small particles called atoms, too small to see with our eyes. ... There are over 100 different types of atoms which are displayed on the periodic table of elements."

Standard deviation. California's new science standards introduce the periodic table in grade 3, while those developed by the National Academy of Sciences discourage use of the terms "atom" and "molecule" with students younger than high school.

Changes in the Carbon Balance of Tropical Forests: Evidence from Long-Term Plots

Oliver L. Phillips,* Yadvinder Malhi,* Niro Higuchi, William F. Laurance, Percy V. Núñez, Rodolfo M. Vásquez, Susan G. Laurance, Leandro V. Ferreira, Margaret Stern, Sandra Brown, John Grace

The role of the world's forests as a "sink" for atmospheric carbon dioxide is the subject of active debate. Long-term monitoring of plots in mature humid tropical forests concentrated in South America revealed that biomass gain by tree growth exceeded losses from tree death in 38 of 50 Neotropical sites. These forest plots have accumulated 0.71 ton, plus or minus 0.34 ton, of carbon per hectare per year in recent decades. The data suggest that Neotropical forests may be a significant carbon sink, reducing the rate of increase in atmospheric carbon dioxide.

Tropical forests contain as much as 40% of the C stored as terrestrial biomass (*1*) and account for 30 to 50% of terrestrial productivity (*2*). Therefore, a small perturbation in this biome could result in a significant change in the global C cycle (*3, 4*). Recent micrometeorological research suggests that there is a net C sink in mature Amazonian forests (*5, 6*), but the ability to draw firm conclusions is hampered by the limited spatial and temporal extent of these measurements. Another approach, applying atmospheric transport models to measured global distributions of CO_2, O_2, and their isotopes (*7*), has yielded conflicting results. We report a third approach to explore the role of mature tropical forests in the global C cycle, namely, the use of permanent sample plots (PSPs). PSPs, established by foresters and ecologists to monitor tree growth and mortality, have the potential to yield C accumulation estimates that are at once both geographically extensive and of high spatial and temporal resolution.

We compiled data on basal area (cross-sectional area of trees per unit ground area) from mature tropical forest plots (*8*) that meet appropriate a priori criteria (*9*). Basal area of trees is a well-substantiated surrogate measure of total biomass in tropical forests (*10*), so changes due to tree growth and mortality provide an effective measure of changes in biomass. We tested for changes in mature tropical forest biomass in each of four nested regions: the humid tropics (153 plots), the humid Neotropics (120 plots), the humid lowland Neotropics (108 plots), and Amazonia (97 plots) (*11*). These plots represent more than 600,000 individual tree measurements tropics-wide.

We conducted two analyses with the information available. For each region, we first calculated the mean rate of change in tree basal area across sites, based on the difference between the initial and final census at each geographically distinct site (*12*). Sites may contain one or more floristically and edaphically similar plots (*13*). In the second analysis, we estimated basal area change as a function of calendar year and derived an estimate of regional net accumulated biomass through time. Data for this approach were derived for each site by first computing differences between each successive census, then by linear interpolation between successive censuses for years when measurements were not taken, and finally for each year by averaging change across all contributing plots. Measurement errors were corrected by comparing multiple measurements of the same tree over time (*14*). Basal area values were converted to aboveground biomass estimates by using an allometric model developed for lowland forest in central Amazonia and by using correction factors to account for the biomass of lianas and small trees (*15*).

Biomass has increased in mature forest sites in the humid Neotropics (1.11 ± 0.54 t ha^{-1} $year^{-1}$; mean ± 95% confidence intervals), the humid lowland Neotropics (1.08 ± 0.59 t ha^{-1} $year^{-1}$), and in Amazonia (0.97 ± 0.58 t ha^{-1} $year^{-1}$) (*16*). The entire pantropical dataset also shows an increase in biomass (0.77 ± 0.44 t ha^{-1} $year^{-1}$), but the signal is dominated by the Neotropical pattern, and there has not been a significant change in Paleotropical sites (tropical Africa, Asia, Australia) (−0.18 ± 0.59 t ha^{-1} $year^{-1}$) (*17*). In the Neotropics (tropical Central and South America), the mean value of biomass change has been positive for most years since widespread PSP monitoring began (*18*). In Amazonia, where most inventories are located, plots have on average gained biomass in most years since at least the late 1970s (Fig. 1). By 1990, mature forest sites in all three nested Neotropical regions had on average accumulated substantial biomass (Fig. 2).

These results show that (i) there is considerable spatial and temporal variability in rates of biomass change, yet (ii) on average,

O. L. Phillips, School of Geography, University of Leeds, Leeds, LS2 9JT, UK. Y. Malhi and J. Grace, Institute of Ecology and Resource Management, University of Edinburgh, Edinburgh, EH9 3JU, UK. N. Higuchi, Departamento de Silvicultura Tropical, Instituto Nacional de Pesquisas da Amazônia, C.P. 478, 69011-970 Manaus, Amazonas, Brazil. W. F. Laurance, S. G. Laurance, L. V. Ferreira, Biological Dynamics of Forest Fragments Project, Instituto Nacional de Pesquisas da Amazônia, C.P. 478, 69011-970, Manaus, Amazonas, Brazil. P. V. Núñez, Umanchata 136, Biodiversidad Amazónica, Cusco, Peru. R. M. Vásquez, Missouri Botanical Garden–Proyecto Flora del Perú, Apartado 280, Iquitos, Peru. M. Stern, Institute of Economic Botany, New York Botanical Garden, Bronx, NY 10458, USA. S. Brown, Department of Natural Resources and Environmental Sciences, University of Illinois, Urbana, IL 61801, USA.

*To whom correspondence should be addressed. E-mail: O.Phillips@geog.leeds.ac.uk (O.L.P); YMalhi@ed.ac.uk (Y.M.)

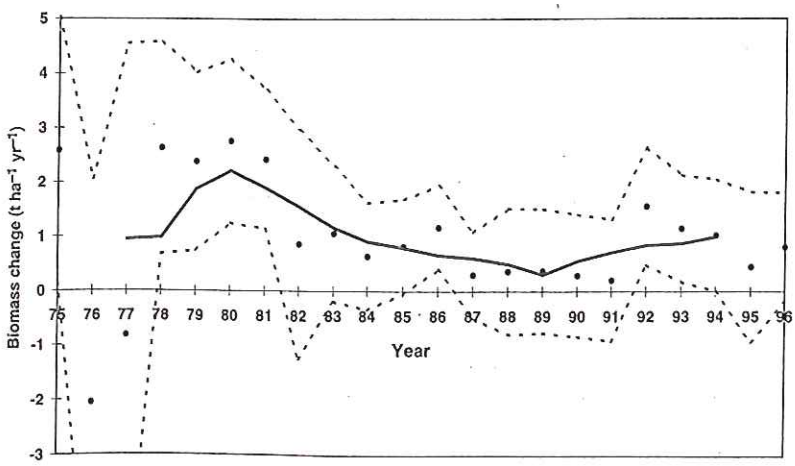

Fig. 1. Annual aboveground biomass change in Amazonian forests, 1975–96. Mean (solid circles), 95% confidence intervals (dotted line), and 5-year moving average (solid line) are shown.

plots have gained biomass, and (iii) the increase has been especially marked in lowland Neotropical sites. There has been no statistically detectable change in biomass in African and Asian plots, but our coverage of these areas (18 sites) is sparser than in the Neotropics (50 sites), so we concentrate our discussion on the Neotropics. If the difference between Neotropical and Paleotropical forests is genuine, it may reflect differing climatic factors or perhaps greater human disturbance in the more densely populated Paleotropics (*19*).

Before extrapolating these results to the biomass of Neotropical forests as a whole, it is important to consider whether the PSPs were representative of the broader region. Neotropical forests are heterogeneous (*20*), and our dataset spans much of the natural variation in Amazonian forests (*21*). The number of extra-Amazonian lowland and montane samples also corresponds to the approximate coverage of each region (*22*). Recent debate (*23*) has centered on two potential problems in monitoring: (i) research activity having a negative impact on tree survivorship and growth and (ii) plots becoming increasingly subject to edge effects as surrounding forest is fragmented (*24*). These effects would increase mortality relative to growth, thus causing a decline in measured biomass—the opposite of our result. A further possibility is that there could be a bias in the PSPs compared to the surrounding forest, by systematic avoidance or underreporting of forests that underwent natural catastrophic disturbances or smaller scale disturbance due to localized tree death. Although it is difficult to quantify such a bias, there is little evidence for it in our dataset (*25*), and the increase in biomass is larger than can be accounted for simply by the dynamics of a few large trees (*26*).

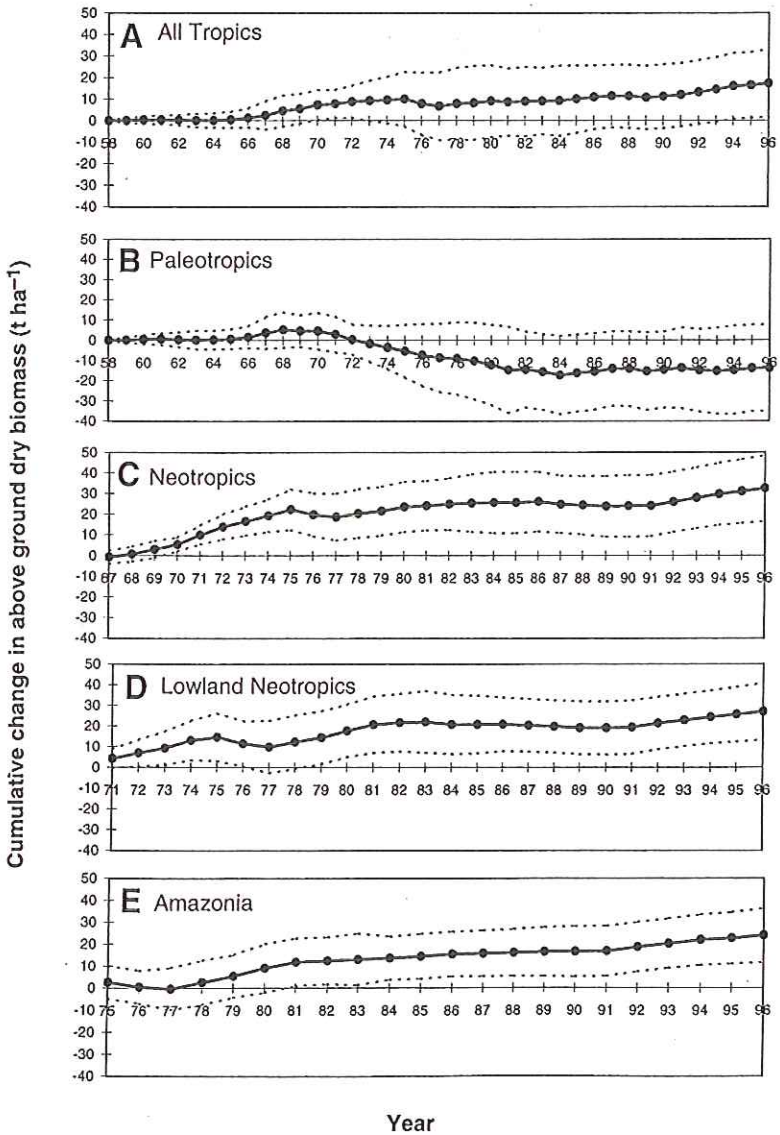

Fig. 2. Cumulative aboveground net biomass change (tons per hectare per year) in humid forests in: (**A**) the Tropics since 1958; (**B**) the Paleotropics (tropical Africa, Asia, Australia) since 1958; (**C**) the Neotropics (tropical Central and South America) since 1967; (**D**) the lowland Neotropics since 1971; (**E**) Amazonia since 1975. Annual mean (solid line) and 95% confidence interval (dotted line) values are based on the cumulative changes in individual sites since the first year and are scaled by a/b, where a = the cumulative time elapsed since the first year and b = the mean monitoring period per site up to each year end.

Our results are therefore indicative of a widespread increase in the biomass of surviving Neotropical forests over recent decades. There are a number of mechanisms that may explain this change: (i) a response to continental-scale cyclical climate change; (ii) recovery from widespread disturbance, either natural or anthropogenic; (iii) enhanced forest productivity due to a secular change in climate or increased nutrient availability.

Because Earth's climate fluctuates, forest stocks of C might be responding to past climatic events. The El Niño–Southern Oscillation (ENSO) may be one long-term driver of cyclical changes in forest dynamics (*27*). In El Niño years, most of Amazonia receives below-normal rainfall (*28*), but our data show that Amazon forests gained biomass before, during, and after the intense 1982–83 ENSO (Fig. 1). It is possible that regional forest biomass is recovering from earlier greater disturbances, either from drought or from the impacts of indigenous peoples who have experienced steep population declines since the 16th century (*29*). The biomass increase could also be a response to recent anthropogenic global change. There is some evidence for an increase in temperate and tropical forest productivity (*30*), and even mature ecosystems may gain biomass if plant productivity is stimulated (*4*). Candidate factors for nutrient fertilization include increasing atmospheric CO_2 (*31*) and increased N and P deposition from Saharan dust (*32*) and biomass burning (*33*).

To estimate regional C sequestration rates, we first converted aboveground biomass into C stocks, using allometric data obtained in central Amazonia (*34*). The increase in biomass on Amazonian plots is equivalent to a net uptake of 0.62 ± 0.37 t C ha^{-1} $year^{-1}$. Multiplying this by the estimated area of humid forest in lowland Amazonia (*22*) produces a mature forest biomass C sink of 0.44 ± 0.26 Gt C $year^{-1}$. Similarly, the estimated annual C sink in lowland Neotropical humid forest is 0.52 ± 0.28 Gt C; it is 0.62 ± 0.30 Gt C for all mature humid neotropical forests. Our method suggests a lower C uptake rate than estimates from eddy covariance studies in Rondônia (1.0 t ha^{-1} $year^{-1}$) (*2*) and near Manaus (5.9 t ha^{-1} $year^{-1}$) (*6*). The discrepancy may reflect the limited spatial and temporal extent of eddy covariance measurements, or else be indicative of significant in-

creases in the necromass and soil pools (*35*), which are not accounted for in our analysis.

Our results suggest that mature Neotropical forest biomass may account for ~40% of the so-called "missing" terrestrial C sink (*36*). Hence, intact forests may be helping to buffer the rate of increase in atmospheric CO_2, thereby reducing the impacts of global climate change. However, the C sink in mature forests appears vulnerable to several factors. There is likely to be an upper limit to the biomass a forest stand can hold. Moreover, deforestation, logging (*37*), increased fragmentation and edge-effect mortality (*23, 24*), regional drying and warming (*38*), and possible intensification of El Niño phenomena (*39*) may limit and even reverse the sink provided by mature forest. A dedicated large network of permanent biomass plots could provide vital insight into the future role of tropical forests in the global C cycle.

References and Notes

1. R. K. Dixon *et al.*, *Science* **263**, 185 (1994).
2. J. Grace, Y. Malhi, N. Higuchi, P. Meir, in *Terrestrial Global Productivity: Past, Present, and Future*, H. A. Mooney, J. Roy, B. Saugier, Eds. (Academic Press, London, in press).
3. A. E. Lugo and S. Brown, *For. Ecol. Manage.* **54**, 239 (1992); S. Brown, J. Sathaye, M. Cannell, P. Kauppi, in *Climate Change 1995: Impacts, Adaptations, and Mitigation of Climate Change, Scientific-Technical Analyses, Contributions of Working Group II to the Second Assessment Reports of the IPCC*, R. T. Watson, M. C. Zinyowera, R. H. Moss, Eds. (Cambridge Univ. Press, Cambridge, 1995), pp. 775–797.
4. J. A. Taylor and J. Lloyd, *Aust. J. Bot.* **40**, 407 (1992).
5. J. Grace *et al.*, *Global Change Biol.* **1**, 1 (1995); J. Grace *et al.*, *Science* **270**, 778 (1995).
6. Y. Malhi *et al.*, *J. Geophys. Res.*, in press.
7. P. Ciais, P. P. Tans, M. Trolier, J. W. C. White, R. J. Francey, *Science* **269**, 1098 (1995); I. G. Enting, C. M. Trudinger, R. J. Francey, *Tellus Ser. B* **47**, 35 (1995); E. R. Hunt *et al.*, *Global Biogeochem. Cycles* **10**, 431 (1996).
8. Sequential basal area data were sourced in three ways: (i) from unpublished plots in Peru, Brazil, and Venezuela censused by the authors and colleagues; (ii) by asking others responsible for monitoring mature plots for permission to use their unpublished data; and (iii) from the literature. Basal area (*BA*, in square meters) is related to diameter (*D*, in meters) by $BA = \Pi (D/2)^2$.
9. Mature tropical forest data were included where living trees ≥10 cm in diameter were measured either at 1.3 m (nonbuttressed trees) or immediately above buttress roots. Sites that experienced natural disturbances before or during the inventory period were generally included, but cyclone-prone forests (such as Puerto Rico or Australia) were excluded to avoid biases in timing; most such plots were either recensused immediately after cyclones hit or else are established in areas recovering from cyclones [see also review by E. V. J. Tanner, J. R. Healey, V. Kapos, *Biotropica* **23**, 513 (1991)]. This exclusion was conservative; biomass increased in the two cyclone-forest sites with published long-term basal area data [T. R. Crow, *ibid.* **12**, 42 (1980); D. I. Nicholson, N. Henry, J. Rudder, *Proc. Ecol. Soc. Aust.* **15**, 61 (1988)]. Plots in forest fragments ≤100 ha and plots that suffered mass mortality by logging or deforestation before or during the inventory period were also excluded.
10. For example, J. M. Pires and G. T. Prance, in *Amazonia*, G. T. Prance and T. E. Lovejoy, Eds. (Pergamon, Oxford, 1985), pp. 109–145; S. Brown, A. J. R. Gillespie, A. E. Lugo, *For. Sci.* **35**, 881 (1989); *Can. J. For. Res.* **21**, 111 (1991); I. Foster Brown, D. C. Nepstad, I. de O. Pires, L. M. Luz, A. S. Alechandre, *Environ. Conserv.* **19**, 307 (1992); A. J. R. Gillespie, S. Brown, A. E. Lugo, *For. Ecol. Manage.* **48**, 69 (1992).
11. "Humid tropics" includes forest receiving >1500 mm precipitation annually; "lowlands" includes forest <500 m above mean sea level; "Amazonia" includes humid forest within the phytogeographical region of Amazonia, encompassing Amazonian Brazil, Colombia, Ecuador, Peru, Bolivia, the Guianas, and contiguous moist forest in Venezuela, excluding nonforest vegetation.
12. Data table and data references are available as supplementary material at the *Science* Web site. (www.sciencemag.org/feature/data/976299.shl)
13. Mean individual plot size per site = 1.87 ha; data from plots <0.2 ha were pooled.
14. Excessive declines or increases in diameter of trees reported in individual censuses indicate human measurement error and were corrected by interpolating between prior and subsequent censuses.
15. The relationship between tree basal area (*BA*, in square meters per hectare) and fresh aboveground biomass of trees ≥10 cm diameter (*AGFB*, in tons per hectare) has the linear form $AGFB = 66.92 + 16.85(BA)$, with $r^2 = 0.85$, based on destructive harvesting of 319 trees at site 9. The relationship was tested and found to be appropriate at another site in eastern Amazonia [T. M. Araujo, N. Higuchi, J. A. Carvalho Jr., *An. Acad. Bras. Cienc.* (1996)]. Correction factors were included for the biomass of trees with diameter <10 cm (× 1.062), on the basis of the biomass-DBH (diameter at breast height) distribution, and for lianas with diameter ≥1 cm (× 1.037), on the basis of liana/tree biomass comparisons in Amazonian forests [E. E. Hegarty and G. Caballé, in *The Biology of Vines*, F. E. Putz and H. E. Mooney, Eds. (Columbia Univ. Press, New York, 1991), pp. 313–336]. Other generally minor components of plant biomass such as stranglers, epiphytes, shrubs, and herbs were not considered. The proportion of water in *AGFB* (40%) was determined from the destructive sampling of 38 trees and the partial sampling of 100 trees at site 9.
16. Neotropics: $n = 50$ sites, 38 with positive change, $P < 0.001$; lowland Neotropics: $n = 45$ sites, 34 with positive change, $P < 0.01$; Amazonia: $n = 40$ sites, 30 with positive change, $P < 0.01$. P values are for two-tailed binomial tests; the one Amazon site with no change was treated as negative change.
17. All tropics: $n = 68$ sites, 48 with positive change, $P < 0.01$; Paleotropics: $n = 18$ sites, 10 with positive change, not significant. P values are for two-tailed binomial tests.
18. For years in which ≥5 sites were monitored, the mean change was positive in 24 of 30 years 1967–96 for the Neotropics ($P < 0.01$), in 21 of 26 years 1971–96 for the lowland Neotropics ($P < 0.01$), in 20 out of 22 years 1975–96 for Amazonia ($P < 0.001$), in 13 of 30 years 1958–87 for the Paleotropics (not significant), and in 36 of 41 years since 1956 for all tropical forests ($P < 0.001$). P values are for two-tailed binomial tests.
19. T. C. Whitmore, in *Tropical Forest Remnants: Ecology, Management and Conservation of Fragmented Communities*, W. F. Laurance and R. O. Bierregaard, Eds. (Univ. of Chicago Press, Chicago, 1997), pp. 3–12.
20. H. Tuomisto *et al.*, *Science* **269**, 63 (1995).
21. Nonflooded forests on low- to medium-fertility pre-Holocene substrates cover 65 to 70% of Amazonia [J. M. Pires, in *Tropical Forest Ecosystems* (UNESCO, Paris, 1978), pp. 607–627] and comprise 70% of our Amazonian sites. Other extensive Amazonian forest types (on alluvial, white sand, and swampy substrates) feature in the dataset in proportion to their region-wide abundance.
22. Estimates of humid tropical forest areas vary according to definition. We use the 1990 area estimates from the Food and Agricultural Organisation [*FAO Forestry Paper 112* (FAO, Rome, 1993)], combining areas described as tropical rain forest, moist deciduous forest, and hill and montane forest to calculate humid Neotropical forest area in the lowlands (7,486,150 km²) and in total (8,705,100 km²). Our estimate of lowland Amazonian forests (7,116,280 km²) is based on combining the lowland humid forest figures for Brazil, Bolivia, Colombia, Ecuador, French Guyana, Guyana, Peru, Suriname, and Venezuela. The area is dominated by the Amazonian hylaea, but also includes small areas of lowland forest along the Pacific and Atlantic coasts.
23. See also R. O. Bierregaard, T. E. Lovejoy, V. Kapos, A. Santos, R. Hutchings, *Bioscience* **42**, 859 (1992); O. L. Phillips, *Science* **268**, 894 (1995); D. Sheil, *ibid.*, p. 894; *For. Ecol. Manage.* **77**, 11 (1995); R. Condit, *Trends Ecol. Evol.* **12**, 249 (1997); L. V. Ferreira and W. F. Laurance, *Conserv. Biol.* **11**, 797 (1997); O. L. Phillips and D. Sheil, *Trends Ecol. Evol.* **12**, 404 (1997); O. L. Phillips, P. Nuñez V., M. Timaná, *Biotropica*, in press.
24. Fragmented Amazonian forests can experience precipitous declines in biomass after isolation [W. F. Laurance *et al.*, *Science* **278**, 1117 (1997)], and edge effects have been suggested to extend up to 1000 m in from forest margins [D. Skole and C. Tucker, *ibid.* **260**, 1905 (1993)]. We excluded a priori any plots in fragments ≤100 ha, but some Neotropical sites are in larger islands or narrow peninsulas of forest (sites 1, 42, 43), are close to forest edges abutting on large areas that have been deforested before or during the monitoring periods (sites 2, 34), or are characterized by both these conditions. The mean rate of biomass change in these sites is −0.42 t ha^{-1} $year^{-1}$.
25. If plots measuring a catastrophic loss were somehow excluded from the study, they would have been done so a priori or post priori. A mechanism for a priori exclusion would be that forest vulnerable to catastrophes is selected against when plots are established, but it is difficult to see what criteria could be used to make such an assessment. For example, while multiple tree-falls covering large areas do occasionally occur, where they will occur is unknowable. Moreover, any such tendency may select against young stands obviously recovering from disturbances (for example, gaps regenerating after local flooding) and bias our results instead to the parts of the landscape gaining C less rapidly. A mechanism for post priori exclusion would be that plots suffering catastrophic losses are abandoned and not reported. However, we are not aware of any cases of abandoning tropical forest plots after catastrophic loss, and monitoring the impacts of such natural catastrophic events would presumably be of extra scientific value [see also (*9*)].
26. As an example, we take the BIONTE study area in central Amazonia where diameter/biomass relationships have been derived for individual tree species. In the BIONTE study plots of 3 ha by 1 ha (site 8), mean biomass is 353 t ha^{-1}. Biomass of the five largest trees was 17.2, 13.0, 9.4, 8.0, and 7.8 t. Thus, the loss of one of these large trees would only represent a loss of 1.6, 1.2, 0.9, 0.8, and 0.8% of the total inventoried biomass (equivalent to 4.9 to 2.2%, respectively, of total biomass in 1 ha). Although some trees are very long-lived [J. Q. Chambers, N. Higuchi, J. P. Schimel, *Nature* **391**, 135 (1998)], the dynamics of the much more numerous smaller trees are more important. In the BIONTE example, the gain of biomass in the 3 ha by 1 ha study between 1980 and 1997 was 90.5 t, which represents the equivalent of 5.3 times the biomass of the single largest tree and is spread throughout the study area. On a wider scale, many of the Neotropical plots have recently experienced very high mortality rates and rapid recruitment of small trees [O. L. Phillips, P. Hall, A. H. Gentry, S. A. Sawyer, R. Vásquez, *Proc. Natl. Acad. Sci. U.S.A.* **91**, 2805 (1994); O. L. Phillips, *Environ. Conserv.* **23**, 235 (1996); O. L. Phillips, P. Hall, S. Sawyer, R. Vásquez, *Oikos* **79**, 183 (1997)], which indicates that Neotropical forest dynamics are not dominated by the behavior of a few giant, slow-growing trees.
27. R. Condit, S. P. Hubbell. R. B. Foster, *Ecol. Monogr.* **65**, 419 (1995); M. Keller, D. A. Clark, D. B. Clark, A. M. Weitz, E. Veldkamp, *Science* **273**, 201 (1996).
28. C. F. Ropelewski and M. S. Halpert, *Mon. Weather Rev.* **115**, 1606 (1987).
29. W. M. Denevan, *Ann. Assoc. Am. Geogr.* **82**, 369 (1992).
30. For example, D. A. Graybill and S. B. Idso, *Global Biogeochem. Cycles* **7**, 81 (1993); M. Becker, T. M. Nieminen, F. Gérémia, *Ann. Sci. For.* **51**, 477 (1994);

O. L. Phillips and A. H. Gentry, *Science* **263**, 954 (1994); R. A. Houghton, *Tellus Ser. B* **48**, 420 (1996); R. F. Keeling, S. C. Piper, M. Heimann, *Nature* **381**, 218 (1996).
31. R. B. McKane, E. B. Rastetter, J. M. Melillo, G. R. Shaver, C. S. Hopkinson, *Global Biogeochem. Cycles* **9**, 329 (1995); Ch. Korner and F. A. Bazzaz, Eds., *Carbon Dioxide, Populations, and Communities* (Academic Press, San Diego, 1996); J. Lloyd and G. D. Farquhar, *Funct. Ecol.* **10**, 4 (1996).
32. R. Swap, M. Garstang, S. Greco, R. Talbot, P. Kallberg, *Tellus Ser. B* **44**, 133 (1992).
33. For example, D. S. Schimel *et al.*, *Global Biogeochem. Cycles* **10**, 677 (1996); P. M. Vitousek *et al.*, *Ecol. Appl.* **7**, 737 (1997). Tropical forest tree growth has been shown experimentally to increase after N and P fertilization [E. V. J. Tanner, V. Kapos, W. Franco, *Ecology* **73**, 78 (1992)].
34. We assumed that: (i) 48% of biomass is in the form of C (based on burning experiments near Manaus, central Amazonia [J. A. Carvalho Jr., J. M. Santos, J. C. Santos, M. M. Leitão, N. Higuchi, *Atmos. Environ.* **29**, 2301 (1995); J. A. Carvalho Jr., N. Higuchi, T. M. Araujo, J. C. Santos, *J. Geophys. Res.* **103**, 13195 (1998)]]; (ii) that the ratio of aboveground biomass to root biomass is 3:1 (the average value of three studies in Brazilian Amazonia [P. Fearnside, *Emissão e Sequestro de CO_2* (Companha Vale do Rio Doce, Rio de Janeiro, 1994), pp. 95–124]], consistent with a global analysis of root biomass allocation [M. A. Cairns, S. Brown, E. Helmer, G. Baumgardner, *Oecologia* **111**, 1 (1997)]; and (iii) that root biomass increased in proportion to aboveground biomass. We ignored C stocks in fine litter, dead wood, and soil, which may also have changed.
35. Although PSP data address the problem of spatial variability that can limit extrapolation of eddy covariance studies, they clearly cannot assess the behavior of necromass and belowground C pools, which might be expected to increase together with biomass. A combination of eddy covariance and biomass studies may provide a useful tool in the future to examine belowground processes.
36. The "missing" sink was recently estimated at ~1.4 Gt [D. S. Schimel, *Global Change Biol.* **1**, 77 (1995)]. By comparison, deforestation in Brazilian Amazonia was estimated to yield a net C emission of 0.34 Gt in 1990 [P. M. Fearnside, in *Biomass Burning in South America, Southeast Asia, and Temperate and Boreal Ecosystems, and the Oil Fires of Kuwait*, J. S. Levine, Ed. (MIT Press, Cambridge, MA, 1996), pp. 606–617]. Deforestation in the whole Neotropics was estimated to yield 0.6 ± 0.3 Gt C annually between 1980 and 1990 [R. A. Houghton, in *Forest Ecosystems, Forest Management and the Global Carbon Cycle*, M. G. Apps and D. T. Price, Eds., *NATO ASI Ser. I Global Environ. Change*, vol. 40 (Springer-Verlag, Heidelberg, Germany, 1996)].
37. W. F. Laurance, *Trends Ecol. Evol.*, in press.
38. E. Salati and C. A. Nobre, *Clim. Change* **19**, 177 (1991); A. Kattenberg *et al.* (1996), *Climate Change* (Intergovernmental Panel on Climate Change/Cambridge Univ. Press, Cambridge, 1995), pp. 285–357.
39. D. Z. Sun, *Geophys. Res. Lett.* **24**, 2031 (1997).
40. We gratefully acknowledge help in Peru from the late A. H. Gentry, as well as M. Aguilar, C. Díaz, C. Grández, N. Jaramillo, M. Jarrell, K. Johnson, D. Milanowski, R. Ortíz, S. Rose, J. Terborgh, A. Vásquez, and the logistical support of INRENA, ACEER, Cuzco Amazonico Lodge, Explorama Tours, Instituto de Investigaciones de la Amazonía Peruana, Peruvian Safaris, Universidad Nacional de la Amazonía Peruana (Iquitos), and Universidad Nacional de San Antonio Abad del Cusco (Cusco and Puerto Maldonado). In Brazil, we acknowledge the help of R. J. Ribeiro, Y. Biot, P. Delamonica, C. Gascon, and other BIONTE and BDFFP project members. We thank J. Terborgh, R. Foster, R. Condit, S. Lao, S. P. Hubbell, M. D. Swaine, D. Nicholson, R. Keenan, T. Richards, J. N. M. Silva, J. P. Veillon, J. Comiskey, and R. Moraes de Jesus for kindly making data available and for other help. Peruvian field research was supported by the American Philosophical Society, National Geographic Society (grant 5472-95), NSF (BSR-9001051), World Wide Fund for Nature (WWF)–U.S./Garden Club of America, Conservation International, the MacArthur and Mellon Foundations, Missouri Botanical Garden, and a Research Fellowship from the U.K. Natural Environment Research Council (NERC). Support for Venezuelan data analysis was provided by a cooperative agreement between the USDA Southern Forest Experiment Station and the University of Illinois (grant 19-91-064). The Biological Dynamics of Forest Fragments Project (BDFFP) was supported by WWF-US, INPA, Smithsonian Institution, and the MacArthur and Mellon Foundations. Work by Y.M., N.H., and J.G. formed part of the Biomass and Nutrient Experiment (BIONTE) and the Anglo-Brazilian Climate Observation Study (ABRACOS), supported by the U.K. Overseas Development Administration in collaboration with the Agencia Brasileira de Cooperação, and aided by a NERC Terrestrial Initiative in Global and Environmental Research (TIGER) grant.

13 January 1998; accepted 11 September 1998

A Large Terrestrial Carbon Sink in North America Implied by Atmospheric and Oceanic Carbon Dioxide Data and Models

S. Fan, M. Gloor, J. Mahlman, S. Pacala, J. Sarmiento, T. Takahashi, P. Tans

Atmospheric carbon dioxide increased at a rate of 2.8 petagrams of carbon per year (Pg C $year^{-1}$) during 1988 to 1992 (1 Pg = 10^{15} grams). Given estimates of fossil carbon dioxide emissions, and net oceanic uptake, this implies a global terrestrial uptake of 1.0 to 2.2 Pg C $year^{-1}$. The spatial distribution of the terrestrial carbon dioxide uptake is estimated by means of the observed spatial patterns of the greatly increased atmospheric carbon dioxide data set available from 1988 onward, together with two atmospheric transport models, two estimates of the sea-air flux, and an estimate of the spatial distribution of fossil carbon dioxide emissions. North America is the best constrained continent, with a mean uptake of 1.7 ± 0.5 Pg C $year^{-1}$, mostly south of 51 degrees north. Eurasia–North Africa is relatively weakly constrained, with a mean uptake of 0.1 ± 0.6 Pg C $year^{-1}$. The rest of the world's land surface is poorly constrained, with a mean source of 0.2 ± 0.9 Pg C $year^{-1}$.

A number of carbon cycle studies conducted in the last decade have indicated that the oceans and terrestrial ecosystems in the Northern Hemisphere absorb atmospheric CO_2 at a rate of about 3 Pg C $year^{-1}$ (*1–3*). Atmospheric CO_2 concentrations in the Northern Hemisphere are about 3 parts per million (ppm, mole fraction in dry air) greater than those in the Southern Hemisphere. Fossil CO_2 is released predominantly at northern latitudes (Table 1), which should result in a north-to-south decrease of 4 to 5 ppm in the concentration of atmospheric CO_2 (*4*). A Northern Hemisphere sink is implied because the observed gradient is smaller than this. The original studies disagreed on whether the sink was predominantly oceanic (*1*) or terrestrial (*2*). Recent studies with atmospheric $^{13}C/^{12}C$ ratios (*5*) and oxygen concentrations (*6*) concluded that the sink is caused primarily by terrestrial biosphere uptake. Other studies demonstrated increased activity of sufficient magnitude by the terrestrial biosphere in northern latitudes: a longer growing season observed in satellite measurements of surface color (*7*) and an increase over time of the amplitude of the annual cycle of atmospheric CO_2 concentrations caused by terrestrial vegetation (*8*).

The partitioning of the Northern Hemisphere terrestrial CO_2 sources and sinks between Eurasia and North America may be estimated by using the west-to-east gradient of atmospheric CO_2 across the continents. The west-east signal is much smaller and more difficult to detect than the north-south signal for two reasons. First, the CO_2 distribution is smoothed more by the relatively rapid zonal atmospheric transport than by the slower meridional transport (weeks instead of ~1 year for interhemispheric exchange). Sec-

S. Fan and J. Sarmiento, Atmospheric and Oceanic Sciences Program, Princeton University, Princeton, NJ 08544, USA. M. Gloor and S. Pacala, Department of Ecology and Evolutionary Biology, Princeton University, Princeton, NJ 08542, USA. J. Mahlman, Geophysical Fluid Dynamics Laboratory–National Oceanic and Atmospheric Administration (NOAA), Princeton University, Post Office Box 308, Princeton, NJ 08542, USA. T. Takahashi, Lamont-Doherty Earth Observatory, Columbia University, Palisades, NY 10964, USA. P. Tans, Climate Modeling and Diagnostics Laboratory, NOAA, Boulder, CO 80303, USA.

*Correspondence should be addressed to the Carbon Modeling Consortium, AOS Program, Princeton University, Princeton, NJ 08544, USA. E-mail: cmc@princeton.edu

ond, atmospheric sampling stations have traditionally been located primarily offshore, away from the largest terrestrial signals to avoid the complexities associated with continental atmospheric boundary layers, the diurnal character of photosynthesis, local fossil fuel emissions, and topography (Fig. 1).

To provide improved estimates of net annual terrestrial sources and sinks, we have developed an inverse model. Let $O(\mathbf{x})$ be the annual-average spatial pattern of atmospheric CO_2 caused by atmospheric transport acting on the sea-air CO_2 flux, and $F(\mathbf{x})$ and $R(\mathbf{x})$ be the corresponding annual-average spatial patterns associated with fossil fuel emissions and the seasonal rectification, respectively (where $\mathbf{x}$ is the spatial coordinate vector). Seasonal rectification results from the correlation between the seasonality of vertical mixing in the atmosphere and the seasonality of photosynthesis and respiration in the land biosphere, which causes gradients in the annual mean CO_2 concentration even when the terrestrial biosphere has no net annual emissions (*9*). Assuming a terrestrial biosphere with no net emissions, the expected annual average spatial pattern of atmospheric CO_2 is $O(\mathbf{x}) + F(\mathbf{x}) + R(\mathbf{x})$. We use the difference between this expected spatial pattern and the observed annual average concentrations of atmospheric CO_2 at sampling stations [$S(\mathbf{x}_j)$ for a station located at $\mathbf{x}_j$] to estimate the magnitude and spatial distribution of terrestrial uptake.

We divide the land surface into N regions and let $b_i(\mathbf{x})$ be the global spatial pattern of atmospheric CO_2 caused by atmospheric transport acting on a standard annual terrestrial uptake of 1 Pg C within the i^{th} region. Then, the total spatial pattern caused by nonzero terrestrial uptake is

$$B(\mathbf{x}) = \sum_{i=1}^{N} \alpha_i b_i(\mathbf{x}) \qquad (1)$$

where α_i is the magnitude in Pg C year^{-1} of terrestrial uptake in the i^{th} region, and is estimated by linear regression (*10*).

We used two separate atmospheric transport models of the Geophysical Fluid Dynamics Laboratory (GFDL) to calculate the expected spatial pattern of atmospheric CO_2. A previous model comparison study showed significant differences in predictions of the fossil CO_2 distribution and rectification effect (*4*). The use of two different models gives us some measure of the sensitivity of the results to differences in the transport model. The Global Chemical Transport Model (GCTM) uses winds generated previously by an atmospheric general circulation model (*11*, *12*). In contrast, the SKYHI model (*12*, *13*) calculates tracer transport at the same time it calculates the winds and subgrid-scale mixing.

To calculate the $O(\mathbf{x})$ function, we used two different estimates of the global spatiotemporal distribution of net sea-air CO_2 flux. OBM is an annual mean sea-air flux from a global ocean biogeochemistry model (*14*). T97 is a seasonally resolved sea-air flux field based on estimates from the more than 2.1 million measurements of the sea-air difference of CO_2 partial pressure (pCO_2) gathered over the last three decades and interpolated by using annual mean ocean currents from OBM (*15*, *16*). Pacific equatorial (10°N to 10°S) observations made during El Niño periods were excluded from the estimate. The data are normalized to 1990. The total sea-air CO_2 flux is larger in OBM than T97 (Table 1). A comparison of model simulations with observations of $\Delta^{14}C$ in the ocean favors the larger uptake of OBM (*17*).

The two atmospheric models and two patterns of sea-air CO_2 flux gave us four possible combinations. To calculate in each case, we ran the atmospheric model with the prescribed pattern of sea-air flux for five annual cycles until the annual average spatial distribution of atmospheric CO_2 reached a steady state.

To calculate $O(\mathbf{x})$, we used data on national fossil fuel consumption distributed with the same spatial distribution as population density (*18*). Using this pattern of release at the surface, we ran each atmospheric model to its steady state as above.

Finally, to calculate $R(\mathbf{x})$ and the $b_i(\mathbf{x})$, a

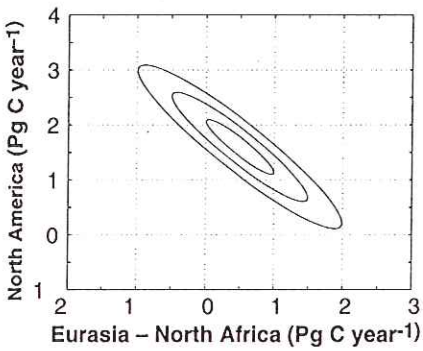

Fig. 2. Inversion uncertainties for North American terrestrial uptake versus Eurasia–North African terrestrial uptake. Ellipses of 1, 2, and 3 SDs are shown.

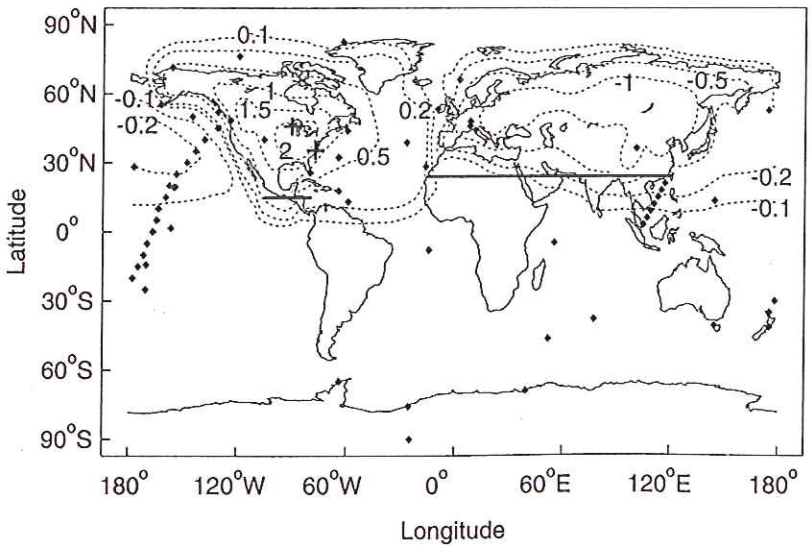

Fig. 1. A map of the atmospheric CO_2 sampling network. Sites are shown as solid diamonds. (The Globalview labels for the Northern Hemisphere stations are given in the legend of Fig. 3). The tall tower sites are shown as crosses. The thick horizontal lines divide the land surfaces into three regions where terrestrial carbon uptake has been estimated: North America, Eurasia–North Africa, and Tropics and Southern Hemisphere. The dotted contour lines show the difference between predicted surface CO_2 concentrations (ppm) with estimated terrestrial uptake and with North American terrestrial uptake set to zero (model results are shown for GCTM with the T97 sea-air fluxes).

Table 1. Regional distribution of fossil CO_2 emissions and sea-air fluxes for 1990. T97 and OBM are two different air-sea flux estimates (see text).

Region	Fossil emissions (Pg C year^{-1})
North America (>15°N)	1.6
Eurasia and North Africa (>24°N)	3.6
Tropics and Southern Hemisphere	0.7
Total	5.9

	Ocean uptake (Pg C year^{-1})	
	T97	OBM
North Atlantic (>15°N)	0.55	0.51
North Pacific (>15°N)	0.29	0.70
Tropics and Southern Hemisphere	0.27	1.04
Total	1.11	2.25

model of the terrestrial biosphere is required. We chose the Carnegie-Ames-Stanford Approach (CASA) model (*19*), because it predicts ecosystem fluxes of CO_2 with a relatively straightforward extrapolation of global satellite imagery (normalized difference vegetation index or NDVI measurements on a 1° grid). We calculated $R(\mathbf{x})$ by running each atmospheric model with surface fluxes from a version of the CASA model (again until a steady state spatial pattern was achieved). To calculate $b_i(\mathbf{x})$, we ran the atmospheric model with no sources or sinks of CO_2 except net primary production (NPP) from the CASA model in only the i^{th} region. This NPP was first rescaled until the annual total was 1 Pg C. Thus, the spatiotemporal distribution of estimated carbon sinks within each terrestrial region is assumed to be proportional to the distribution of NPP, but this assumption has little impact on the results (see below).

The atmospheric CO_2 data we used cover the 1988 to 1992 period at a subset of 63 sampling stations (*20*) taken from the GLOBALVIEW database (*21*) compiled with methods as described by Masarie and Tans (*22*) (Fig. 1). Before 1988 there were fewer sampling stations; a separate study indicates that even with optimal placement, which the present data set does not have, a minimum of about 10 stations per region is necessary to obtain estimates with useful accuracy (*23*).

We first defined three regions, North America north of 15°N, Eurasia–North Africa north of 24°N, and all other land to the south (Fig. 1). Subsequently, North America was separated into temperate and boreal zones at approximately the evergreen–broadleaf ecotone (51°N). Additional divisions lead to prohibitively large estimation errors. In particular, there are insufficient atmospheric stations in the Southern Hemisphere to separate Africa from South America.

North America is constrained by the atmospheric observations on three sides of the continent (Fig. 1); a large North American terrestrial uptake is estimated in all four combinations of atmospheric models with sea-air CO_2 flux data (Table 2). Most of the North American terrestrial uptake (70 to 100%) is estimated to be in the broadleaf region south of 51°N. If the North American terrestrial uptake were zero (that is, all of the Northern Hemisphere's net terrestrial uptake were in Eurasia), the models would predict an average increase of atmospheric CO_2 of more than 0.3 ppm from stations located between 10°N and 60°N in the North Pacific to those in the North Atlantic. A North American terrestrial sink is implied by the data because the observed gradient shows a decrease from North Pacific to North Atlantic of about 0.3 ppm.

We estimated standard deviations for the estimates of terrestrial uptake by propagating independent, identically distributed Gaussian station errors (Table 2). The ellipses in Fig. 2 suggest that the total Northern Hemisphere sink is well constrained, and that the partitioning between North America and Eurasia–North Africa is more weakly constrained. However, the terrestrial carbon sink in North America is sufficiently large to be detected with the present observational and model constraints.

None of these error estimates include systematic errors such as differences between GCTM and SKYHI and between T97 and OBM. We use the differences between estimates from the four models (Table 2) as an admittedly limited assessment of the magnitude of systematic errors. The range of estimates produced by the differences between the models is small for North American uptake and intermediate for Eurasian uptake. Estimates of Eurasia–North African terrestrial uptake obtained with SKYHI are 0.7 to 0.9 Pg C $year^{-1}$ lower than those obtained with GCTM. SKYHI has a more rapid vertical mixing than GCTM and predicts lower fossil CO_2 at stations in the mid-latitude Northern Hemisphere, which implies a lower terrestrial uptake in the region.

The systematic errors are especially large for estimates of the terrestrial uptake in the tropics and Southern Hemisphere, as evidenced by the large differences among the estimates shown in Table 2. The wide range of 2.0 Pg C $year^{-1}$ in these estimates is caused by a combination of factors. Differences between OBM and T97 account for 1.3 Pg C $year^{-1}$ (Table 2). Differences between SKYHI and GCTM account for 0.7 Pg C $year^{-1}$.

An alternative four-region inversion, with only one region in North America but two in Eurasia–North Africa, yields marginal evidence of a weak uptake in boreal Eurasia (0.6 ± 0.4 Pg C $year^{-1}$) with a more uncertain, but generally compensating source in temperate Eurasia (-0.5 ± 0.7 Pg C $year^{-1}$). However, five-region inversions (with separate temperate and boreal regions in both North America and Eurasia–North Africa) were unstable, with standard errors of estimates as large as 1.4 Pg C $year^{-1}$. The only stable regions were temperate and boreal North America and the union of temperate and boreal Eurasia–North Africa, for which terrestrial uptake estimates and errors similar to those in Table 2 were obtained.

Detection of the terrestrial CO_2 uptake in North America and in Eurasia can be improved

Table 2. Estimated terrestrial carbon uptake for 1988 to 1992. Positive terrestrial carbon uptake is a flux out of the atmosphere. GCTM and SKYHI are the two atmospheric GCM models and T97 and OBM are the two air-sea flux estimates used in the inversions (see text).

Source region	Terrestrial uptake (Pg C $year^{-1}$)				SD of the estimate* (Pg C $year^{-1}$)	Mean and summary SE† (Pg C $year^{-1}$)	Forest area (10^9 ha)
	GCTM		SKYHI				
	T97	OBM	T97	OBM			
			Three-region inversion				
North America	1.6	1.7	1.7	1.7	±0.5	1.7 ± 0.5	0.8
Eurasia and North Africa	0.5	0.5	−0.4	−0.2	±0.5	0.1 ± 0.7	1.2
Tropics and Southern Hemisphere	0.1	−1.1	0.9	−0.5	±0.1	−0.2 ± 0.9	2.1
Total	2.2	1.1	2.2	1.1	–	–	–
			Four-region inversion				
North America							
Boreal	0.4	−0.1	0.5	0.1	±0.3	0.2 ± 0.4	~0.4
Temperate	1.2	1.7	1.2	1.3	±0.4	1.4 ± 0.5	~0.4
Eurasia and North Africa	0.6	0.7	−0.4	0.0	±0.5	0.2 ± 0.7	1.2
Tropics and Southern Hemisphere	0.0	−1.3	0.9	−0.4	±0.1	−0.2 ± 0.9	2.1
Total	2.2	1.1	2.2	1.1	–	–	–

*The SD of the estimate was found by assuming that the Gaussian variance equals χ^2/q ($q = 63$) (*10*), and that data errors from different stations are independent. SDs of estimates obtained with T97 include the sampling uncertainty for oceanic CO_2 exchange (*15*), but those obtained with OBM include no oceanic uncertainty. However, the contribution of T97 error to the total uncertainty is small. †This is the mean of the estimates from the four combinations of atmospheric and oceanic models. The SE is $\sqrt{\sigma^2+V^2}$, where σ is the SD from the adjacent column and V is the SD of the four estimates in the first four columns.

with atmospheric measurements within or near the continents. If the North American uptake were zero, the CO_2 mixing ratios over eastern North America should increase by over 2 ppm (Fig. 1), which would make that the best place to detect a source or sink proportional to NPP. Data are available from two extremely tall towers (>400 m) within this region (crosses in Fig. 1) for a period later than the 1988 to 1992 interval considered here. Analyzed with a completely different method, these data are consistent with the existence of a large sink in North America (*24*).

A detailed summary of the present data that constrain the North American sink (Fig. 3) illustrates how near the limit of detection the signal is. The fit of the model to the observations in the optimal case is better than 0.5 ppm at most locations in both the Pacific and Atlantic. Zeroing out the North American sink lowers the Pacific model predictions and raises the Atlantic, thereby reversing the west-to-east gradient from −0.3 to +0.3 ppm (Fig. 3; note particularly that the Atlantic predictions go from being relatively well centered around the observations to having five stations well above the observations). Zeroing out Eurasia raises the model predictions in the Pacific and lowers them in the Atlantic.

We tested the sensitivity of the solutions to individual stations by removing stations one at a time. In all cases the removal of a station had an impact of ≤0.3 Pg C year^{-1}, with most being near zero. The exclusion of Sable Island (44°N60°W) from the data set (*20*) does have a substantial impact on the inversion results. Including it in the GCTM-T97 and -OBM inversions reduces the North American terrestrial uptake by 0.4 to 0.5 Pg C year^{-1} and shifts it to Eurasia–North Africa.

The estimate of North American terrestrial uptake was found to be insensitive to large changes in the North Pacific uptake, and only weakly related to the Southern Ocean (south of 54°S) uptake. In contrast, for an incremental change in the temperate North Atlantic sink, the estimate of North American terrestrial uptake changes by ~1.5 times as much in the opposite direction. However, the temperate North Atlantic sink had to be increased by about a factor of 5, from 0.3 to 1.4 Pg C year^{-1}, to eliminate the North American sink (*25*).

A large North American terrestrial uptake was estimated consistently for a range of spatiotemporal patterns assumed for the terrestrial uptake (*26*), because subcontinental terrestrial signals are sufficiently smoothed at most of the air-sampling stations (Fig. 1).

Suppose that our mean estimate of the North American terrestrial carbon sink were distributed uniformly over the forest region south of 51°N (Table 2) (*27*); then, the per unit area forest uptake would be 3 to 4 t C ha^{-1} year^{-1}. This is in the uppermost range of some independent measurements at local sites (*28*, *29*). A lower estimate on the order of 1 Pg C year^{-1} for the North American terrestrial uptake, which is near the lower error bound of 1 SD (Fig. 2), would be in better agreement with the local measurements. However, even our low estimate is much larger than the 0.2 to 0.3 Pg C year^{-1} uptake estimated on the basis of forest inventory data for North American forests (*30*, *31*), which did not take full account of carbon storage in soils, wetlands, and lakes (*32*).

The terrestrial uptake in North America is at least partly due to regrowth on abandoned farmland and previously logged forests (*30*, *31*). Numerous field and laboratory studies have suggested that terrestrial uptake is currently enhanced by anthropogenic nitrogen deposition [0.2 to 2.0 Pg C year^{-1} globally, with much of this in the Northern Hemisphere (*33*, *34*)], CO_2 fertilization [0.5 to 2.0 Pg C year^{-1} globally, with most of this in the tropics (*33*)], and global warming [mostly in the north temperate zone (*8*, *35*)]. On the other hand, warming might also have reduced terrestrial uptake by enhancing decomposition (*29*, *36*).

Although the inversion results indicate that the North American terrestrial uptake is large enough to be detected with current data and model constraints, its magnitude remains uncertain and its cause unknown. Thus, the immediate implication of our results is the need for additional constraints of four kinds: (i) intensive atmospheric sampling and ecological field studies to indentify the location and cause of North American terrestrial CO_2 uptake; (ii) new atmospheric measurements to constrain estimates for Eurasia, South America, Africa, and Australia; (iii) studies to better characterize oceanic CO_2 uptake, particularly in the Southern Hemisphere; and (iv) reduced uncertainty in atmospheric transport modeling.

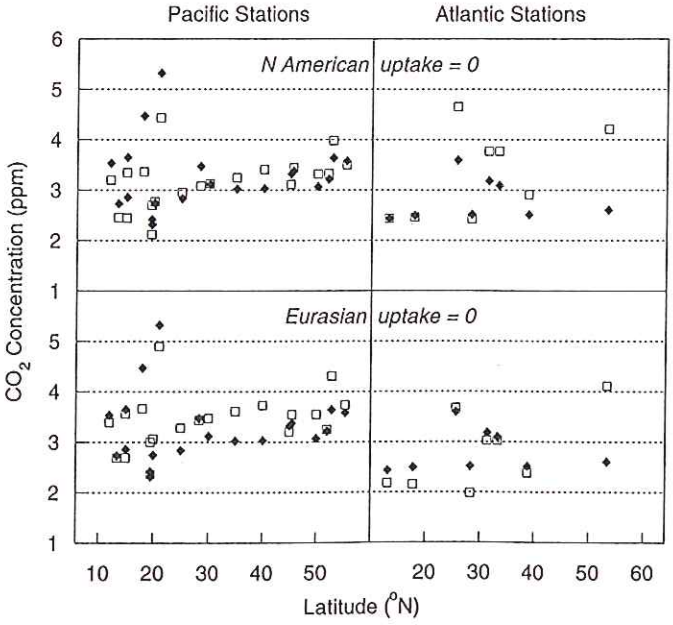

Fig. 3. Comparison of model-predicted atmospheric CO_2 concentrations (□) with observations (1988—1992 average) (◆) at Pacific and Atlantic sampling locations between 10° to 60°N. Model results are shown for GCTM with T97 sea-air fluxes, and with North American terrestrial uptake set to zero (that is, all Northern Hemisphere terrestrial uptake placed in Eurasia–North Africa), or Eurasia–North African terrestrial uptake set to zero (that is, all Northern Hemisphere terrestrial uptake placed in North America). Although the Mace Head station (in the Atlantic at 53.3°N) is an outlier in all plots, it has little impact on the inversion estimates because predictions at this station are affected only slightly by zeroing North American or Eurasian uptake. Data are shown for the following locations, with their latitude (°N) and longitude (a negative sign indicates °W and a positive sign indicates °E) in parentheses: AVI (17.75, −64.75), AZR (38.75, −27.08), BME (32.37, −64.65), BMW (32.27. −64.88), CBA (55.20, −162.72), CMO (45.48, −123.97), CSJ (51.93, −131.02), GMI (13.43, 144.78), IZO (28.30, −16.48), KEY (25.67, −80.20), KUM (19.52, −154.82), MHT (53.33, −9.90), MID (28.22, −177.37), RPB (13.17, −59.43), SHM (52.72, 174.10), STP (50.00, −145.00), pocn15 (15.00, −160.00), pocn20 (20.00, −158.00), pocn25 (25.00, −154.00), pocn30 (30.00, −148.00), pocn35 (35.00, −143.00), pocn40 (40.00, − 138.00), pocn45 (45.00, −131.00), scsn12 (12.00, 111.00), scsn15 (15.00, 113.00), scsn18 (18.00, 115.00), and scsn21 (21.00, 117.00).

References and Notes

1. C. D. Keeling, S. C. Piper, M. Heimann, in *Aspects of Climate Variability in the Pacific and the Western Americas, AGU Monograph 55*, D. H. Peterson, Eds. (American Geophysical Union, Washington, DC, 1989), pp. 305–363.
2. P. P. Tans, I. Y. Fung, T. Takahashi, *Science* **247**, 1431 (1990).
3. I. G. Enting and J. V. Mansbridge, *Tellus* **43B**, 156 (1991).
4. R. M. Law *et al.*, *Global Biogeochem. Cycles* **10**, 783 (1996).
5. P. Ciais, P. P. Tans, M. Trolier, J. W. C. White, R. J. Francey, *Science* **269**, 1098 (1995).
6. R. F. Keeling, S. C. Piper, M. Heimann, *Nature* **381**, 218 (1996).
7. R. B. Myneni, C. D. Keeling, C. J. Tucker, G. Asrar, R. R. Nemani, *ibid.* **386**, 698 (1997).
8. C. D. Keeling, J. F. S. Chin, T. P. Whorf, *ibid.* **382**, 146 (1996); J. T. Randerson, M. V. Thompson, T. J. Conway, I. Y. Fung, C. B. Field, *Global Biogeochem. Cycles* **11**, 535 (1997).
9. A. S. Denning, I. Y. Fung, D. Randall, *Nature* **376**, 240 (1995).

10. The sizes of the terrestrial sources and sinks can be estimated by solving for the values of α_i that minimize the sum

$$\chi^2 = \sum_{j=1}^{q} [B(x_j) + O(x_j) + F(x_j) + R(x_j) - S(x_j)]^2 \quad (2)$$

where q is the number of atmospheric sampling stations. In practice, it is convenient to reference all concentrations in the sum of squares to the value at the South Pole, and then solve for the values of α by using singular value decomposition [W. H. Press, B. R. Flannery, S. A. Teukolsky, W. T. Vetterling, *Numerical Recipes* (Cambridge Univ. Press, New York, 1992)] with a mass conservation constraint [G. H. Golub and C. F. V. Loan, *Matrix Computations* (Johns Hopkins Univ. Press, Baltimore, 1990)] that requires the terrestrial biosphere to balance all the other sources minus sinks.

11. J. D. Mahlman and W. J. Moxim, *J. Atmos. Sci.* **35**, 1340 (1978); H. Levy, J. D. Mahlman, W. J. Moxim, *J. Geophys. Res.* **87**, 3061 (1982).
12. Meridional and vertical transport in both GCTM and SKYHI have been evaluated against observations of radon-222, krypton-85, and CFC-11. The original comparison with radon-222 observations led to the implementation of a more aggressive vertical mixing scheme in SKYHI that improved the simulation of this tracer. A recent model comparison study with SF_6 shows that both SKYHI and GCTM do well at simulating marine boundary-layer concentrations, although the continental concentrations may be too high (A. S. Denning *et al.*, *Tellus*, in press).
13. K. Hamilton, R. J. Wilson, J. D. Mahlman, L. J. Umscheid, *J. Atmos. Sci.* **52**, 5 (1995).
14. J. L. Sarmiento, R. Murnane, C. L. Quéré, *Philos. Trans. R. Soc. London Ser. A* **348**, 211 (1995); R. Murnane, J. L. Sarmiento, C. L. Quéré, *Global Biogeochem. Cycles*, in press.
15. T. Takahashi *et al.*, *Proc. Natl. Acad. Sci. U.S.A.* **94**, 8992 (1997).
16. The sea-air flux is calculated by taking the product of the sea-air pCO_2 difference and a climatic wind speed–dependent estimate of the gas exchange flux based on the oceanic inventory of bomb radiocarbon [R. Wanninkhof, *J. Geophys. Res.* **97**, 7373 (1992)]. Most of the difference between OBM and T97 in global oceanic uptake (0.8 Pg C $year^{-1}$) occurs in the tropics and Southern Hemisphere (Table 1), where the spatiotemporal coverage of measurements used in T97 and tracer data used for model evaluation is very uneven. The recent completion of the World Ocean Circulation Experiment will greatly improve the coverage.
17. U. Siegenthaler and J. L. Sarmiento, *Nature* **365**, 119 (1993).
18. R. J. Andres, G. Marland, I. Fung, E. Matthews, *Global Biogeochem. Cycles* **10**, 419 (1996).
19. C. S. Potter *et al.*, *ibid.* **7**, 811 (1993). The CASA model does not consider the effect of biomass burning and biospheric emissions of hydrocarbons. Oxidation of hydrocarbons leads to the formation of CO, which is further oxidized to CO_2 in the atmosphere. Because the biomass burning and CO oxidation sources of CO_2 are not modeled, they are effectively treated here as part of the biospheric respiration of CASA.
20. The GLOBALVIEW-CO2 1996 database has a total of 66 stations. Tae-Ahn Peninsula and Westerland were excluded because they are strongly contaminated by local fossil CO_2 sources that are difficult for the coarse resolution models to simulate in sufficient detail. Sable Island was excluded because it appears that the data may have a positive bias (K. Higuchi, personal communication). The following procedures were followed in calculating annual averages of model simulations for comparison with observations. (i) Sampling of models at coastal stations was moved out to sea by one grid cell in order to avoid inadvertent terrestrial contamination resulting from the coarse resolution of the atmospheric general circulation models (GCMs). (ii) All other sampling was done at the nearest grid cell to the station. (iii) Four stations were sampled by wind sectors in order to match as closely as possible the way that the actual sampling is done: Cape Grim, Tasmania (180° to 270°); Cape Meares, Oregon (210° to 330°); Key Biscayne, Florida (30° to 160°); and Mace Head, Ireland (210° to 300°).
21. GLOBALVIEW-CO2, *Cooperative Atmospheric Data Integration Project—Carbon Dioxide* (NOAA/CMDL, Boulder, CO, 1996), CD-ROM; also available via anonymous FTP to ftp.cmdl.noaa.gov, Path: ccg/co2/GLOBALVIEW.
22. K. A. Masarie and P. P. Tans, *J. Geophys. Res.* **100**, 11,593 (1995).
23. M. Gloor, S.-M. Fan, S. Pacala, J. L. Sarmiento, in preparation.
24. P. S. Bakwin, P. P. Tans, D. F. Hurst, C. Zhao, *Tellus*, in press.
25. The mean North Atlantic air-sea pCO_2 difference measured by T97 is 20 ± 5 μatm. Increasing the temperate North Atlantic air-sea flux to 1.4 Pg C $year^{-1}$ would require an increase in the air-sea pCO_2 difference to about 90 μatm, or a 4.5 times increase of the gas exchange coefficient [which is already about twice as large as other commonly used estimates (*17*)], or some combination of the two. Tans *et al.* discussed this issue in their study (*2*). An independent constraint on the North Atlantic sink is the anthropogenic carbon inventory estimate obtained from analysis of observations of dissolved inorganic carbon [N. Gruber, J. L. Sarmiento, T. F. Stocker, *Global Biogeochem. Cycles* **10**, 809 (1996)]. This estimate is almost identical to the OBM simulations (which agree with T97 in the North Atlantic).
26. There was little impact on the estimates when the terrestrial uptake was assumed to be proportional to the heterotrophic respiration in the CASA model (*19*), which has very different temporal patterns from the NPP. In another case, the terrestrial uptake was assumed to be invariable with season and to be uniform within each of five regions (separate boreal and temperate regions in Eurasia–North Africa and North America, and the rest of land surfaces combined). The estimates of total terrestrial uptake for North America and for Eurasia–North Africa were well constrained and remained essentially unchanged from those shown in Table 2 (averaged over the four cases) even with this radical assumption.
27. M. Williams, in *World Deforestation in the Twentieth Century*, R. J. Richards and R. P. Tucker, Eds. (Duke Univ. Press, Durham, NC, 1988), pp. 211–229; K. Power, personal communication.
28. S. C. Wofsy *et al.*, *Science* **260**, 1314 (1993); M. L. Goulden, J. W. Munger, S. M. Fan, B. C. Daube, S. C. Wofsy, *ibid.* **271**, 1576 (1996); S. Greco and D. D. Baldocchi, *Global Change Biol.* **2**, 183 (1996).
29. M. L. Goulden, J. W. Munger, S.-M. Fan, B. C. Daube, S. C. Wofsy, *Science* **279**, 214 (1998).
30. R. A. Birdsey *et al.*, *USDA Forest Service, Productivity of America's Forests and Climate Change* (1995); D. P. Turner, G. J. Koerper, M. E. Harmon, J. J. Lee, *Ecol. Appl.* **5**, 421 (1995).
31. D. Schimel *et al.*, in *Climate Change 1995*, J. T. Houghton *et al.*, Eds. (Cambridge Univ. Press, Cambridge, 1996), pp. 76–86
32. R. F. Stallard, *Global Biogeochem. Cycles* **12**, 231 (1998).
33. J. M. Melillo, I. C. Prentice, G. D. Farquhar, E.-D. Schulze, O. E. Sala, in (*31*), pp. 447–481.
34. D. W. Schindler and S. E. Bayley, *Global Biogeochem. Cycles* **7**, 717 (1993); R. J. M. Hudson, S. A. Gherini, R. A. Goldstein, *ibid.* **8**, 307 (1994); A. R. Townsend, B. H. Braswell, E. A. Holland, J. E. Penner, *Ecol. Appl.* **6**, 806 (1996); E. A. Holland *et al.*, *J. Geophys. Res.* **102**, 15849 (1997).
35. N. Nicholls, *et al.*, in (*31*), pp. 133–192; R. B. Myneni, S. O. Los, C. J. Tucker, *Geophys. Res. Lett.* **23**, 729 (1996).
36. A. Dai, I. Y. Fung, *Global Biogeochem. Cycles* **7**, 599 (1993).
37. This research was carried out as part of the Carbon Modeling Consortium (CMC), which is supported by the Office of Global Programs and Geophysical Fluid Dynamics Laboratory of the NOAA. We acknowledge support from the Department of Energy. Stimulating discussions with our colleagues in the CMC and elsewhere is gratefully acknowledged, with particular appreciation to P. Bakwin, D. Baker, and M. Bender. L. Bruhwiler, R. Hemler, H. Levy, and W. Moxim provided advice on the GCTM and SKYHI simulations, T. Hughes helped access the OBM results, and C. Field provided the CASA simulation results.

29 May 1998; accepted 15 September 1998

North Atlantic Oscillation Dynamics Recorded in Greenland Ice Cores

C. Appenzeller,* T. F. Stocker, M. Anklin

Carefully selected ice core data from Greenland can be used to reconstruct an annual proxy North Atlantic oscillation (NAO) index. This index for the past 350 years indicates that the NAO is an intermittent climate oscillation with temporally active (coherent) and passive (incoherent) phases. No indication for a single, persistent, multiannual NAO frequency is found. In active phases, most of the energy is located in the frequency band with periods less than about 15 years. In addition, variability on time scales of 80 to 90 years has been observed since the mid-19th century.

The North Atlantic oscillation (NAO) is one of the Northern Hemisphere's major multiannual climate fluctuations and typically is described with an index based on the pressure difference between Iceland and the Azores (*1*). On multiannual time scales, variations in the NAO have a strong impact on North Atlantic and European climate (*2*) and also on the recent surface temperature warming trend in the Northern Hemisphere (*3*). In recent decades the winter index remained predominantly in a positive state, and there is evidence that during this period the variability might have increased (*4*). Analysis of various NAO indices (*5*) showed

C. Appenzeller and T. F. Stocker, Climate and Environmental Physics, University of Bern, Sidlerstrasse 5, CH-3012 Bern, Switzerland. M. Anklin, Department of Hydrology and Water Resources, University of Arizona, Tucson, AZ 85721, USA.

*To whom correspondence should be addressed. E-mail: christof.appenzeller@climate.unibe.ch